

Optimal adaptive testing for epidemic control: combining molecular and serology tests

D. Acemoglu¹, A. Fallah², A. Giometto³, D. Huttenlocher², A. Ozdaglar²,
F. Parise^{*4}, S. Pattathil²

¹Department of Economics, Massachusetts Institute of Technology (MIT)

²Department of Electrical Engineering and Computer Science, MIT

³School of Civil and Environmental Engineering, Cornell University

⁴Department of Electrical and Computer Engineering, Cornell University

Abstract

The COVID-19 crisis highlighted the importance of non-medical interventions, such as testing and isolation of infected individuals, in the control of epidemics. Here, we show how to minimize testing needs while maintaining the number of infected individuals below a desired threshold. We find that the optimal policy is adaptive, with testing rates that depend on the epidemic state. Additionally, we show that such epidemic state is difficult to infer with molecular tests alone, which are highly sensitive but have a short detectability window. Instead, we propose the use of baseline serology testing, which is less sensitive but detects past infections, for the purpose of state estimation. Validation of such combined testing approach with a stochastic model of epidemics shows significant cost savings compared to non-adaptive testing strategies that are the current standard for COVID-19.

1 Introduction

A large literature in mathematical epidemiology has studied how to control and eradicate diseases by means of therapeutics and vaccinations, [Nowzari et al., 2016, Behncke, 2000]. However, the influenza pandemic of 1918 and the current COVID-19 pandemic underscore the difficulty of such eradication in the case of virulent viruses, and have necessitated measures to reduce transmissions, for example with the use of face masks [Chu et al., 2020], social distancing and costly lockdown measures [Flaxman et al., 2020, Bertuzzo et al., 2020] [Di et al., 2020]. Another powerful tool to limit transmissions is early identification of infected individuals and epidemic hot-spots in local communities, which can both be accomplished by testing [Grassly et al., 2020, OECD, 2020]. Nevertheless, during the COVID-19 pandemic testing resources have proven to be limited and expensive in much of the world [AACC, 2020, Apuzzo and Gebredikan, 2020, Mervosh and Fernandez, 2020, Pullano et al., 2020]; in the US, lack of testing capacity not only helped spread the virus but also led to the underestimation of the severity of the pandemic in the first half of 2020, [Fink and Baker, 2020]. This crucial role of testing notwithstanding, the question of how limited testing resources can be deployed to optimally control the spread of a pandemic has attracted relatively little systematic attention.

In this paper, we derive an optimal (dynamic) testing strategy in an SIR (Susceptible, Infected, Recovered) model of epidemics. Because undetected individuals may pass the

*Corresponding author: F. Parise (fp264@cornell.edu), D. Acemoglu (daron@mit.edu), A. Fallah (afallah@mit.edu), A. Giometto (giometto@cornell.edu), D. Huttenlocher (huttenlocher@mit.edu), A. Ozdaglar (asuman@mit.edu), S. Pattathil (sarathp@mit.edu). We acknowledge support from the C3.AI grant. Authors are listed in alphabetical order.

disease to others and may be more likely to develop serious symptoms requiring hospitalization, we start by assuming that the number of undetected infected individuals has to be kept below a maximum i_{\max} at all times. We show that the optimal testing strategy takes a simple form: the testing rate has to be time-varying in order to satisfy the constraint, and takes the form of a *most rapid approach path*, [Spence and Starrett, 1975]. Namely, there is no testing until undetected infections reach i_{\max} , after which testing resources are used to keep infections at the threshold i_{\max} until infections decline naturally, bringing the pandemic to an effective close. The intuition for this result is that it is not worth using testing resources to keep undetected infections strictly below i_{\max} so long as the pandemic is still ongoing and infections cannot be brought down to zero. Hence, the best approach is to let the infection reach the threshold and then keep it there with a time-varying testing policy. Note that such optimal time-varying strategy is state-dependent, that is, the level of testing is dependent on the epidemic state (the current number of infected, susceptible and recovered individuals).

The second contribution of our paper starts by recognizing that the epidemic state needed to implement the aforementioned optimal testing strategy is typically hard to know precisely, as highlighted by the early stages of COVID-19 spread in the US. In fact, the most common qPCR tests for COVID-19, which are molecular tests based on detection of the virus' genetic material via quantitative polymerase chain reaction, may be ill-suited to obtain such aggregate information. These tests identify infected individuals only during a short window of time. For example, according to [Kucirka et al., 2020] the probability of COVID-19 detection via qPCR is above 75% in a window of roughly a week within active cases, while [Roche, 2020] gives a three weeks window for detectability of cases via qPCR. In contrast, serology tests, which detect antibodies produced by the immune system in response to current and past infections, identify infections during a longer window [Kubina and Dziejic, 2020], but are typically less sensitive and thus received relatively less attention in the epidemic control literature. These problems are unlikely to be confined to COVID-19 and would probably recur in the event of future pandemics. To systematize these observations we study the effectiveness of both types of tests for identifying the epidemic state and find that *serology tests*, which have lower sensitivity but are faster, cheaper and can reveal past infections, offer a better alternative than qPCR-like tests (from here on termed *molecular tests*), which have high accuracy but a short-window of detection. Namely, we show that if the transmission rate in the SIR model is time-varying, then the epidemic state cannot be identified—is not observable—with molecular tests alone. Intuitively, just observing the flow of current infections may not be sufficient to distinguish the nonlinear dynamic evolution of the system due to different initial conditions versus different time-varying trajectories of transmission rates. Serology testing overturns this result, however, by providing a cheap way of estimating the stocks of past infected and recovered individuals. This is despite the fact that serology tests may have significant Type II errors because of low sensitivity (especially in the first stage - 0 to 6 days - of infection, [Roche, 2020]). Indeed, we find that Type II errors, which can be very costly when the purpose is to diagnose individual infections, are not problematic for the purpose of estimating the epidemic state (which is aggregate information). For such purpose, detection of recovered individuals is a more important feature than high sensitivity. Hence, serology tests are an ideal complement to molecular tests for the purpose of estimating aggregate infections—an intuition that is formally established by our mathematical analysis.

In addition to our main analysis, we consider two important extensions. First, we study a variant of our baseline model of optimal testing in which both undetected and detected infections have to be kept below a maximum threshold. In this case, the optimal testing strategy is more complex. Nevertheless, we establish that the basic insights from our baseline analysis generalize to this problem. Second, we recognize that in reality

the dynamics of epidemics are intrinsically stochastic. To confirm the robustness of the proposed approach, we apply our testing methodology to a stochastic continuous-time Markov chain model of epidemics and develop an extended Kalman filter [Khalil, 2015] to estimate the epidemic state in the presence of stochasticity. To this end, we exploit an expansion of the master equation governing the probability distribution of the Markov chain model [van Kampen, 2007, Gardiner, 2009] to derive a description of the epidemic dynamics in terms of a Langevin equation, whose mean coincides with the deterministic SIR model used for computing the optimal testing strategy. The covariance matrix of the noise term in the Langevin equation (which can be explicitly characterized as a function of the epidemic state) is then given as input to the extended Kalman filter to optimally incorporate new observations in the model predictions.

Our paper is related to the growing literature on SIR models, especially applied to the recent COVID-19 pandemic. Classic references on the SIR model and its applications to model epidemics include [Kermack and McKendrick, 1927, Daley and Gani, 2001, Diekmann and Heesterbeek, 2000, Keeling and Rohani, 2011, Andersson and Britton, 2012]. Additionally, see [Pastor-Satorras et al., 2015] for a review of models of epidemic processes over networks and [Anderson and May, 1992, Nowzari et al., 2016] for analysis and control of epidemic models. Several papers developed more general compartmental models for analyzing the spread of COVID-19 and examining the effects of interventions (see e.g., [Gatto et al., 2020, Atkeson, 2020, Stock, 2020, Cashore et al., 2020, Zhang et al., 2020, Chinazzi et al., 2020]). Other papers, such as [Paré et al., 2017, Hota and Sundaram, 2019, Paré et al., 2020, Hota and Gupta, 2020] analyzed the spread of epidemics over both time-varying and static networks.

Our work is more closely connected to a smaller literature that considers testing within this framework. [Alvarez et al., 2020, Acemoglu et al., 2020a, Brotherhood et al., 2020] consider testing in the context of optimal lockdown policies in SIR models (in the latter two papers with explicit recognition of heterogeneities across different age groups). Neither of these papers studies optimal testing, nor discusses the problem of identifying the underlying epidemic state, which is assumed to be known in this branch of the literature. [Acemoglu et al., 2020b] considers optimal testing in a simple model of disease percolation, but their focus is on the countervailing effects that testing creates by discouraging social distancing among certain groups of individuals. Moreover, their analysis is simplified by focusing on a non-SIR percolation model that enables explicit characterization and they do not discuss the issue of estimating the underlying epidemic state. [Drakopoulos and Randhawa, 2020] studies settings where accurate tests are not available in abundance. They show that moderately good tests provide enough information to have a positive social outcome, and that it is not optimal to wait for tests with very high accuracy. Similarly, [Larremore et al., 2020] compared molecular and antigen tests and found that test sensitivity is less important than testing frequency for screening purposes. [Kraay et al., 2020] suggests the use of serology testing to allow seropositive individuals (i.e., individuals with immunity) to increase their level of social interaction. They conclude through extensive simulations that serology testing has the potential to mitigate the impacts of the COVID-19 pandemic while also allowing a substantial number of individuals to safely return to social interactions and to the workplace. Information about the epidemic state of individuals obtained through both qPCR and serology tests is used in [Li et al., 2020a] to derive disease-dependent lockdown policies. [Vespignani et al., 2020] highlights the need for integrating seroepidemiological data into transmission models to reduce the uncertainty in the parameter estimates of clinical severity and transmission dynamics. [Behncke, 2000] studies the optimal testing policy when the objective is a weighted combination of the cost of infection and testing with no constraints on the state variables. They show that the optimal testing policy takes the maximal value until some time and

then zero after. The key novelty of our work is to suggest the combined use of serology testing for the purpose of state estimation with molecular testing for optimal containment of the number of infected within a desired thresholds, together with an analytic derivation of the optimal adaptive testing rates.

In characterizing optimal controls in an SIR framework, our paper is related to a few other papers that study optimal lockdown policies in SIR models. These include [Miclo et al., 2020], which provides an analytical characterization of optimal lockdown policies in a setting where suppression is costly and there is an upper bound on the number of infections, representing a constraint on intensive care unit resources. Another related paper in this regard is [Kruse and Strack, 2020] which studies optimal social distancing measures to minimize a combination of the total health and economic cost of the infected population and the cost of reducing the transmission rate. The key difference of our work is that we focus on testing as a means to identify and isolate infected individuals instead of lockdown policies that impose a degree of isolation to an entire community.

Finally, because of its analytical focus, our paper is distinguished from a large number of recent papers that analyze intervention policies numerically (see e.g., [Zaman et al., 2008, Sharma and Samanta, 2015, Di Giamberardino and Iacoviello, 2017, Farboodi et al., 2020], [Gollier and Gossner, 2020], [Berger et al., 2020] among others). As detailed in the discussion section, we believe that the theoretical insights generated from our analysis of the SIR model highlight fundamental mechanisms and properties related to the use of testing as a tool for controlling an epidemic, that can then be generalized and refined to more sophisticated models of specific epidemics as typically done in the numerical literature above.

2 Results

2.1 Optimal adaptive testing strategies

We model the progression of the epidemic in a population via a Susceptible-Infected-Recovered (SIR) model with three compartments corresponding to susceptible, infected and recovered individuals. Testing is introduced in the model by partitioning the infected compartment into infected individuals that have not yet been detected and are free to circulate, which we term infected-undetected (I_u), and infected individuals that have been detected and are therefore separated from the general population (e.g., quarantined), which we term infected-detected (I_d) (see Fig. 1A). Infected-undetected individuals infect susceptible ones with possibly time-varying transmission rate $\beta(t)$, denoting the number of contacts per unit time multiplied by the probability that a contact leads to infection. For the purpose of controlling the epidemics, we assume that molecular testing (such as qPCR) is performed at rate $\theta(t)$ and has sensitivity η , i.e., infected individuals who get tested are detected with probability η . Individuals that test positive for the infection are quarantined and moved to the infected-detected compartment. Infected individuals become recovered with rate γ . The corresponding model equations are:

$$\begin{aligned}
 \frac{ds(t)}{dt} &= -\beta(t)s(t)i_u(t) \\
 \frac{di_u(t)}{dt} &= \beta(t)s(t)i_u(t) - \gamma i_u(t) - \eta\theta(t)i_u(t) \\
 \frac{di_d(t)}{dt} &= \eta\theta(t)i_u(t) - \gamma i_d(t) \\
 \frac{dr(t)}{dt} &= \gamma i_u(t) + \gamma i_d(t),
 \end{aligned} \tag{1}$$

where small letters denote the fraction of individuals in each compartment. We assume that the population size is constant with time, thus the last equation is redundant since $r = 1 - s - i_u - i_d$.

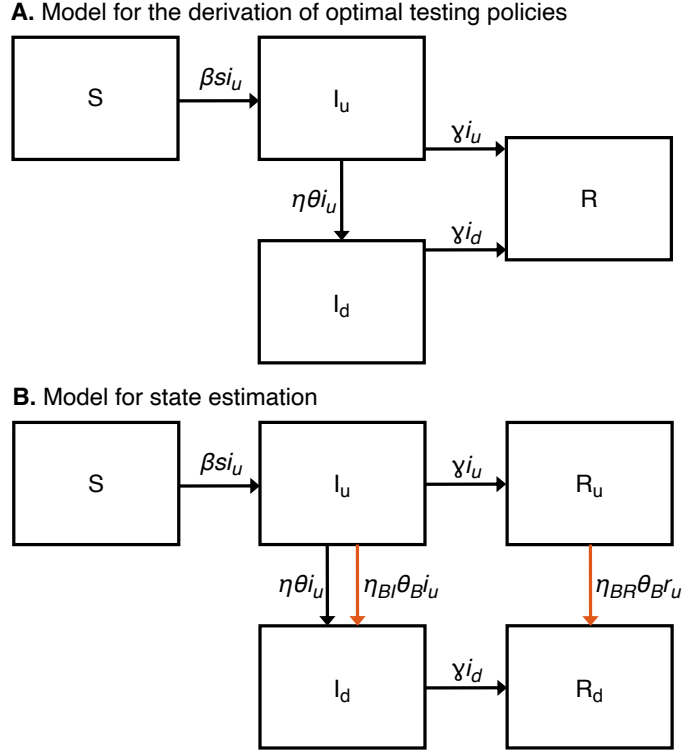


Figure 1: The deterministic epidemiological models used for the derivation of optimal testing policies (A) as discussed in Section 2.1 and for state estimation (B) as discussed in Section 2.2. Individuals in the population are divided in compartments according to their epidemiological state. In (A), Susceptible individuals (S) are infected via contact with infected-undetected individuals (I_u), which either transition to the infected-detected (I_d) compartment if they are tested positive for infection, or to the Recovered (R) compartment if they recover from the infection before being tested positive. Infected-detected individuals also recover from the infection. In (B), infected-undetected individuals (I_u) can transition to the infected-detected state by being tested positive via either adaptive molecular testing or baseline testing. Infected-undetected individuals can also transition to the recovered-undetected (R_u) compartment, if they recover from the infection before being tested positive or displaying symptoms. With serology baseline testing, recovered-undetected individuals can transition to the recovered-detected compartment (R_d) if they are tested positive for past infection. Infected-detected individuals transition directly to the recovered-detected compartment when they recover from the infection. Transitions between compartments are indicated along with the corresponding rates, orange arrows indicate transitions due to serology testing.

Subject to these dynamics, we aim at solving the following constrained optimization problem:

$$\begin{aligned} \min_{\theta(\cdot) \geq 0} \quad & \int_{t=0}^{\infty} \theta(t) dt \\ \text{such that:} \quad & i_u(t) \leq i_{\max} \quad \forall t. \end{aligned} \quad (2)$$

In words, our goal is to design the optimal adaptive testing rate to minimize the total number of tests needed while controlling the epidemic so that the fraction of infected-undetected individuals always remains below a desired threshold $i_{\max} \ll 1$. This constraint

is motivated by two considerations. First, infected-undetected individuals circulate freely in the society and infect others, and thus a high number of such individuals would lead to a rapid takeoff in infections. Second, because they do not receive care, undetected infected individuals may later develop severe complications, and may need emergency intensive care unit (ICU) capacity, which has proven to be in short supply during the COVID-19 pandemic. The appropriate level of i_{\max} is a policy choice, and depends on several factors, including whether policymakers are intending to keep the reproduction rate of the pandemic below one and the maximum surge capacity of ICU resources.

Our first main result provides a complete characterization of the optimal adaptive policy for problem (2). For simplicity we here discuss the case when the transmission rate β is constant (i.e., $\beta(t) = \beta$ for all times). In this case, we say that the system reaches *herd immunity* when the epidemic state is such that $s(t) = \gamma/\beta$, as from that time on the number of infected-undetected individuals decreases even without testing. We prove an analogous theorem with time-varying monotonic $\beta(t)$ in the Supplementary Materials.

Theorem 1. *The optimal testing policy $\theta^\dagger(t)$ for problem (2) with dynamics as in Eq. (1) and constant transmission rate β is described in three phases:*

1. While $i_u(t) < i_{\max}$, do not test, i.e., set $\theta^\dagger(t) = 0$.
2. After $i_u(t)$ reaches i_{\max} , test with time-varying rate $\theta^\dagger(t) = (\beta s(t) - \gamma)/\eta$.
3. Once herd immunity is reached, stop testing, i.e., set $\theta^\dagger(t) = 0$.

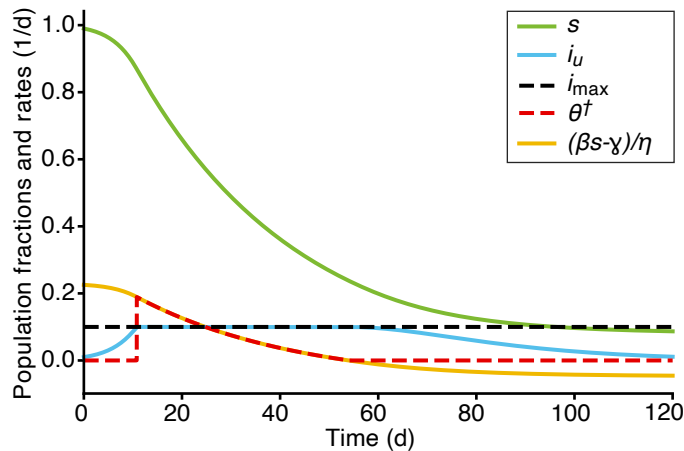


Figure 2: Illustration of the optimal testing policy for problem (2). The green and light-blue curves are, respectively, the fractions of susceptible and infected-undetected individuals in the population. The fraction of infected-undetected i_u is kept below the constraint i_{\max} (black, dashed line) at all times by the optimal adaptive testing policy (red, dashed curve), which is equal to zero until i_u reaches i_{\max} , is then equal to $(\beta s(t) - \gamma)/\eta$ (yellow curve) until herd immunity is reached (i.e., when $s(t) = \gamma/\beta$), and is equal to zero afterwards. For illustration purposes, we set $i_{\max} = 0.1$ and $\eta = 1$, the other parameters are as in Table 1.

As illustrated in Fig. 2, the optimal policy for problem (2) starts testing only once the constraint on i_u is attained, and then sets a time-varying rate $(\beta s(t) - \gamma)/\eta$ such that $di_u(t)/dt = 0$, keeping the fraction of infected-undetected individuals constant at the threshold i_{\max} until herd immunity is reached, after which there is no need for further testing as the epidemic tends naturally towards extinction. Intuitively, given that no testing is needed once herd immunity is reached, the optimal policy takes the form of

the most rapid approach path introduced in [Spence and Starrett, 1975] to reach herd immunity as fast as possible, while satisfying the i_{\max} constraint. The testing policy detailed above leads to the highest number of infected-undetected individuals by employing no testing until undetected infections reach i_{\max} and then utilizing testing resources to keep the infections at this threshold, thus guaranteeing the most rapid feasible path to herd immunity.

2.2 State Estimation

The optimal adaptive testing policy $\theta^\dagger(t)$ derived in the previous section depends on knowledge of the *aggregate epidemic state*, i.e., the values of s , i_u , i_d and r at all times. In practice, because this information is not readily available, the state of the epidemic must be estimated from detected infections. Additionally, the policy makers must know the model parameters. While many of such parameters are related to properties of the disease, the transmission rate is a function of people’s behavior [Weitz et al., 2020], is typically time-varying and needs to be estimated from data. This is a nontrivial problem, since the dynamics induced by the SIR model is highly nonlinear and a given path of infections can be due to different $\beta(t)$ trajectories coupled with different initial conditions.

To address these problems, we propose the use of *baseline testing* with a constant rate θ_B to complement the *adaptive testing* policy derived above, see Fig. 3. Importantly, the objective of baseline testing is not to control the epidemic, but rather to collect enough data to robustly estimate the state of the epidemic and the parameter $\beta(t)$. The policy maker can then use the estimated state and parameter to implement the optimal adaptive policy discussed in Section 2.1.

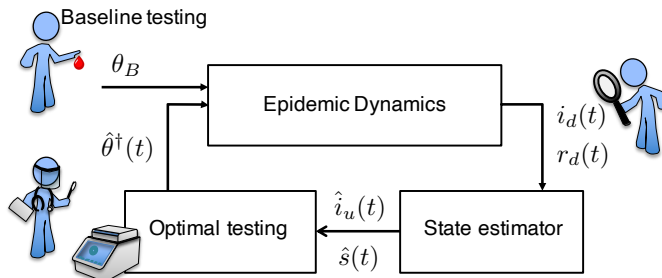


Figure 3: Schematic of the proposed procedure. Measurements of detected-infected and detected-recovered individuals $(i_d(t), r_d(t))$ as defined in Eq. (3) obtained via baseline testing with rate θ_B are used to estimate the aggregate epidemic state $(\hat{s}(t), \hat{i}_u(t))$, which is then used to compute the optimal adaptive testing rate $(\hat{\theta}^\dagger(t))$ according to the results of Theorem 1 (the hat symbol denotes the fact that the optimal testing rate is evaluated as a function of the estimated state). The objective of adaptive testing is to contain the fraction of infected-undetected individuals below the desired threshold i_{\max} .

We next argue that state estimation may be infeasible with molecular testing, which is highly sensitive but detects infections only during a short window of time. Intuitively, detection of current infections from molecular testing is not always sufficient to identify whether a given trajectory of infections is due to a particular time path of $\beta(t)$ coupled with a given set of initial conditions, or to a different time path of transmission coupled with a different set of initial conditions. In contrast, such identification is always possible with baseline serology testing.

To illustrate these points, we consider a more detailed model where we partition the recovered population into recovered-undetected (R_u), consisting of individuals who had the disease but are not recorded as having immunity (because they were not diagnosed

with either test) and recovered-detected (R_d), which consists of individuals that are known to have immunity because they were either detected during their illness or at a later time (via serology testing). Correspondingly, we consider an augmented model that includes both adaptive and baseline testing with different sensitivities (Fig. 1B). All individuals are tested via adaptive molecular testing with rate $\theta(t)$ and sensitivity η , and via baseline testing with sensitivity η_{BI} for the detection of current infections and η_{BR} for the detection of past infections. The model equations read:

$$\begin{aligned}
\frac{ds(t)}{dt} &= -\beta(t)s(t)i_u(t) \\
\frac{di_u(t)}{dt} &= \beta(t)s(t)i_u(t) - \gamma i_u(t) - \eta\theta(t)i_u(t) - \theta_B\eta_{BI}i_u(t) \\
\frac{di_d(t)}{dt} &= \eta\theta(t)i_u(t) + \theta_B\eta_{BI}i_u(t) - \gamma i_d(t) \\
\frac{dr_u(t)}{dt} &= \gamma i_u(t) - \theta_B\eta_{BR}r_u(t) \\
\frac{dr_d(t)}{dt} &= \gamma i_d(t) + \theta_B\eta_{BR}r_u(t),
\end{aligned} \tag{3}$$

where the last equation is redundant since $r_d = 1 - s - i_u - i_d - r_u$.

We use the more detailed model in Eq. (3) to study the system's observability, that is, the question of whether an outside observer or policymaker can estimate the underlying state from detected cases. We prove that even when $i_d(t)$ is observed perfectly and continuously in time but there is no detection of recovered individuals, the underlying state cannot always be estimated (see Lemma 1 in the Materials and Methods Section 4.3). Instead, we prove that when serology testing is used, which allows the correct reconstruction of the time path of both $i_d(t)$ and $r_d(t)$ via observations of both ongoing and past infections, the underlying state can always be estimated (see Lemma 2 in the Materials and Methods Section 4.3). This result does not depend on the frequency of baseline testing, nor on the exact sensitivity of serology testing.

2.3 Extensions

In the previous sections we presented a rigorous analysis of optimal testing and observability for a simple yet insightful deterministic SIR model. Such results are derived under the assumption of perfect and continuous time observations. We next discuss some extensions to account for non-idealities encountered in practice.

First, we consider a model where individuals are detected not only via the testing program but also because they may become symptomatic. Specifically, we assume that infected-undetected individuals may develop symptoms and thus become infected-detected with rate κ (this leads to an additional flow from infected-undetected to infected-detected with rate κ as detailed in Eq. (S4) in the Supplementary Materials). Accordingly, we consider a variant of the original optimization problem where the constraint is imposed on the *total* number of infected individuals, instead of infected-undetected individuals only. We also impose a constraint on the maximum testing rate, modeling daily limitations in processing capacity. Overall, this results in the following extended optimal control problem:

$$\begin{aligned}
&\min_{\theta(\cdot) \geq 0} \int_{t=0}^{\infty} \theta(t) dt \\
&\text{such that: } i_u(t) + i_d(t) \leq i_{\max} \quad \forall t \\
&\qquad\qquad \theta(t) \leq \theta_{\max} \quad \forall t.
\end{aligned} \tag{4}$$

To find the optimal adaptive testing policy $\theta^*(t)$ for the extended problem of Eq. (4), we adopted a numerical approach using the interior point optimizer library within the

GEKKO optimization suite [Beal et al., 2018, Wächter and Biegler, 2006]. The optimal testing policy, computed numerically using parameters taken from the literature on the COVID-19 epidemic (see Materials and Methods Table 1 and Section 4.7) is shown in Fig. 4. Remarkably, the optimal adaptive testing policy for the extended optimization

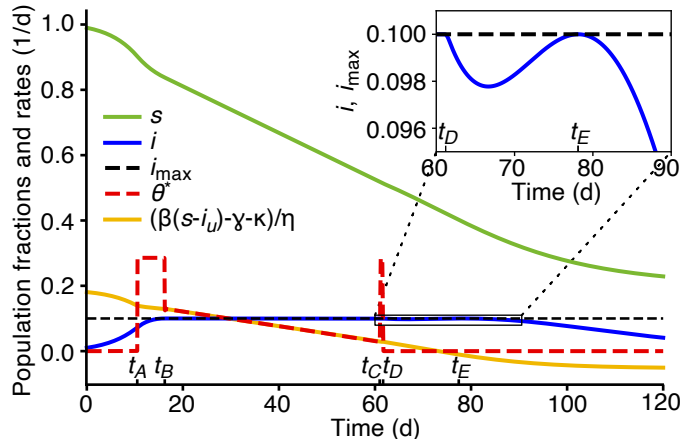


Figure 4: Optimal testing strategy for the extended problem (4). The green and blue curves are, respectively, the fractions of susceptible and infected individuals in the population, respectively. The black, dashed line represents the constraint on the total fraction of infected individuals, $i = i_u + i_d \leq i_{\max}$. The optimal testing policy (red, dashed curve) is equal to zero at first, switches to its maximum value θ_{\max} at time t_A , such that $i_u + i_d$ reaches the constraint i_{\max} with zero derivative at time t_B . Between times t_B and t_C , the optimal testing policy is equal to $(\beta(s(t) - i_u(t)) - \gamma - \kappa)/\eta$ (yellow curve), which keeps $i_u + i_d = i_{\max}$. At time t_C , the optimal testing policy switches back to θ_{\max} until time t_D , after which it is equal to zero. The times t_C and t_D are such that, after t_D , the total fraction of infected individuals grows initially, reaching the constraint i_{\max} tangentially (inset), and then decreases to zero. The switching times can be computed analytically, given the initial condition (as discussed in the Supplementary Materials). For illustration purposes, we set $i_{\max} = 0.1$ and $\eta = 1$, while the other parameters are as in Table 1.

problem of Eq. (4) follows the same principle as the optimal testing policy for the original optimization problem of Eq. (2), that is, it aims at keeping the constrained quantity (i_u for Eq. (2) and $i_u + i_d$ for Eq. (4)) at the threshold i_{\max} for as long as possible, in order to bring the epidemic as fast as possible to a point after which it naturally goes to extinction. Two differences arise in the testing policy that optimizes the modified problem (4). First, in the original problem, one can afford to delay testing right until the time at which i_u reaches the constraint i_{\max} . This is possible because in the original model the first derivative of the constrained quantity, $di_u/dt = i_u(\beta s - \gamma - \eta\theta)$, depends explicitly on the testing frequency θ , and thus one can set the testing rate to $\theta = (\beta s - \gamma)/\eta$ to instantaneously ensure $di_u/dt = 0$. In the extended model, instead, the first derivative of the constrained quantity $i_u + i_d$ does not depend directly on the testing frequency θ . Therefore, one cannot instantaneously impose $d(i_u + i_d)/dt = 0$ and thus testing must start before the constrained quantity $i_u + i_d$ reaches the threshold i_{\max} . The optimal testing policy thus switches from $\theta = 0$ to $\theta = \theta_{\max}$ at a time t_A (for which $i_u(t_A) + i_d(t_A) < i_{\max}$) such that $i_u + i_d$ reaches i_{\max} with zero derivative at time $t_B > t_A$ (Fig. 4). After time t_B , the optimal testing strategy switches to a frequency that maintains $i_u + i_d$ at the i_{\max} value (the specific rate can be computed from equating the second derivative of $i_u + i_d$ to zero). Second, $i_u + i_d$ can naturally decrease even before herd immunity if $i_d > 0$. For this reason, towards the end of the epidemic the optimal testing policy for the extended problem of Eq. (4) adopts a second phase with maximal testing frequency θ_{\max} that decreases i_u and increases i_d up

to a point when, if testing is stopped, $i_u + i_d$ naturally remains below the threshold i_{\max} for all subsequent times (it increases initially but again reaches the threshold tangentially, see inset of Fig. 4). The switching times can be characterized analytically as discussed in the Supplementary Materials.

Next, we allow the dynamics of the epidemic to be governed by a stochastic process rather than a deterministic (albeit time-varying) one. This is, of course, more realistic given the stochastic nature of transmissions and the time-varying and stochastic transition of individuals across different compartments. Additionally, we assume that observation of detected cases happens at discrete time instants (e.g. daily) instead of continuously. To deal with this type of non-idealities and stochasticity in our state estimation, we propose the use of a state-estimator which, given observations at discrete time instants t_k , produces estimates of the state of the system (denoted by \hat{s} , \hat{i}_u , \hat{i}_d , \hat{r}_u , \hat{r}_d), which can then be used to implement the adaptive testing policy. For the purpose of this analysis, we assume that β is known and constant, and use an extended Kalman filter with state constraints as state estimator (Materials and Methods Section 4.5) coupled with a system size expansion of the master equation governing the probability distribution of the stochastic model to derive the dependence of process noise on the epidemic state and population size (Materials and Methods Section 4.4). Extensions to unknown and time-varying β are discussed in the Supplementary Materials Section S.5. To validate our procedure in the presence of non-idealities, we used a receding horizon implementation $\hat{\theta}^*$ of the optimal testing policy derived for the deterministic SIR model (see Materials and Methods Section 4.6). Fig. 5A shows the performance of the state estimator and of the adaptive testing policy for multiple stochastic realizations with $\theta_B = 1/14 \text{ d}^{-1}$ (where d stands for day). The extended Kalman filter provides good estimates (black, dashed curves in Fig. 5C-D) of the real state of the epidemic (blue and orange curves), which lies within the confidence bounds of the estimate. In addition, the time-varying testing rate implemented using the estimated state is effective in maintaining the number of infected individuals around the desired threshold $I_{\max} = Ni_{\max}$ (where N is the population size). Fluctuations of order \sqrt{N} around such threshold are to be expected as the epidemic is simulated as a stochastic, Markov process (Materials and Methods Section 4.4). Finally, we show that the mean of the receding horizon testing policy, computed across realizations of the stochastic model of epidemics, follows the optimal policy derived for the deterministic SIR model (Fig. 5B).

3 Discussion

A major lesson from the recent COVID-19 crisis is that, in the absence of comprehensive vaccines and therapeutic solutions, rapid testing and isolation become crucial tools to contain the spread of a pandemic. In this paper, we developed an approach to determine an optimal testing strategy, relevant especially when there are scarce or expensive testing resources.

Our approach has two basic pillars. First, we showed that, in the context of a classic SIR model, when the epidemic state in terms of infected, recovered and susceptible individuals is known and the objective can be formulated as keeping the number of undetected infections below a certain threshold, then the optimal testing strategy takes a simple form, similar to a most rapid approach path. In particular, there should be no testing until the aforementioned threshold is reached, and thereafter, testing resources should be used to keep infections at this threshold until herd immunity is reached and the epidemic starts disappearing naturally. The standard molecular tests, which have high accuracy, are crucial for this result, because they enable the identification and isolation of infected individuals.

The second pillar of our approach turns to the identification of the epidemic state. Our

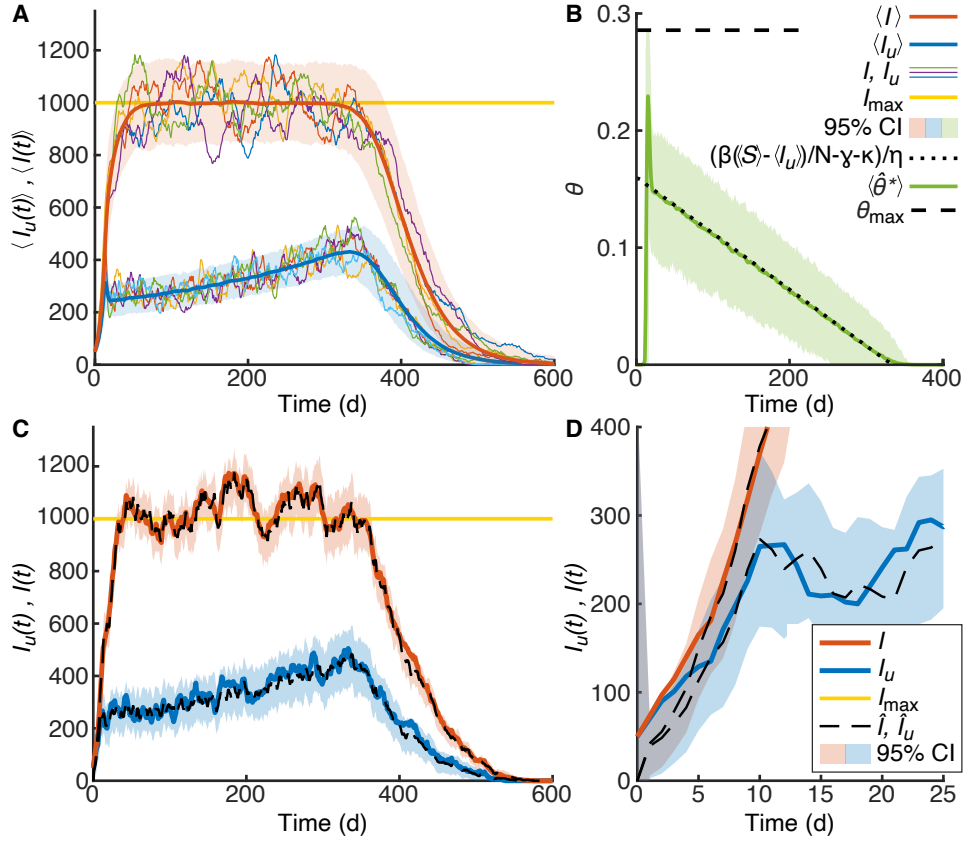


Figure 5: Control of stochastic trajectories by using a receding horizon version of the optimal testing policy θ^* in combination with baseline serology testing with rate $\theta_B = 1/(14 \text{ days})$. Panel A shows the mean number of infected-undetected individuals $\langle I_u(t) \rangle$ (blue, thick curves), the mean total number of infected individuals $\langle I(t) \rangle$ (orange, thick curves) across 500 realizations and $I_u(t)$, $I(t)$ in five, randomly selected stochastic trajectories (solid, thin lines). Note that capital letters denote absolute numbers instead of fractions of individuals. Colored bands are 95% empirical confidence intervals and the thick, yellow lines show the value of I_{\max} . Panel B shows the mean molecular time-varying testing rate in the simulations (thick, green curve) and its 95% confidence interval. The dotted, black line shows $(\beta(\langle S \rangle - \langle I_u \rangle)/N - \gamma - \kappa)/\eta$, which is the functional form of the optimal adaptive testing rate $\theta^*(t)$ for the deterministic SIR model in the interval $[t_B, t_C]$ (Eq. S11). The black, dashed line shows the maximum testing rate θ_{\max} . Panel C shows the number of infected-undetected individuals $I_u(t)$ (blue curve) and the total number of infected individuals $I = I_u(t) + I_d(t)$ (orange curve) in a single realization. The estimated number of infected-undetected individuals $\hat{I}_u(t)$ and estimated total number of infected individuals $\hat{I}(t)$ are shown with black, dashed curves. The 95% confidence intervals for $\hat{I}_u(t)$ and $\hat{I}(t)$ computed using the predicted variance estimated according to the extended Kalman filter are shown as colored bands. The infected threshold value I_{\max} is shown as a yellow line. Panel D shows a zoom of the initial phases of the epidemic highlighting the accuracy of the Kalman filter estimates. Model parameters and initial conditions are as in the Materials and Methods Table 1 and Section 4.7.

optimal testing policy crucially depends on such knowledge, but where does this knowledge come from? We tackle this question by adopting a state estimation framework, where the underlying state is unknown but can be estimated from the sequence of infections and additional information obtained from testing. Though molecular tests are also useful in this context (because they reveal the trajectory of infections), our main result in this part is that this information by itself is not sufficient for identifying the underlying state. This is because the dynamics of the SIR model are highly nonlinear and dependent on initial conditions, and it is not always possible to tell apart whether a given sequence of infections is due to one of many time-varying paths of transmission rates coupled with different initial conditions. Instead, we showed that serology testing which is lower-accuracy, cheaper and longer-range (in terms of estimating past infections) can be useful to disentangle this information.

More specifically, we proposed a two-pronged approach in which baseline serology testing is used to collect information about the state of the epidemic, and the more costly and sensitive molecular testing is adaptively deployed based on such information (Fig. 3). Our analysis formalizes the notion that serology offers advantages as a baseline testing tool not only because of cost benefits, but also because it conveys information about past infections, which proves fundamental to correctly and timely estimate the state of the epidemic. We then showed that, based on information about the state of the epidemic, optimal adaptive molecular testing can be adopted and implemented.

Inevitably for a mathematical analysis based on a stylized model, our approach simplified many aspects of the problem. Our extensions dealt with two such aspects. First, we showed that similar insights apply in the context of an SIR model in which both detected-infected and undetected-infected numbers have to be kept below a certain threshold. Second, our state estimation techniques apply even when we are dealing with a stochastic model of epidemics.

Our analysis suggests that there are tangible gains from the proposed approach. Fig. 6 shows that our two-pillar approach with state estimation plus optimal testing can lead to significant reductions of overall cost with respect to constant testing strategies, leading to up to 60% cost reduction for the parameters we investigated.

In concluding, we make three additional remarks. First, optimality of the proposed approach is claimed in terms of the problems formulated in Eqs. (2) and (4) where the only epidemic constraint comes from keeping infections below a desired threshold i_{\max} . Strategies that achieve such an objective are typically classified as “containment strategies”, since their objective is to contain the disease to a state that can be handled by the health system. This is very different from “eradication strategies” where instead the objective is to eradicate the disease as fast as possible. It is important to note that the more costly constant testing strategy detailed in the Materials and Methods Section 4.2 would lead to faster eradication of the disease than the adaptive strategy suggested here, but testing would need to continue indefinitely to ensure that outside infections would not create further waves, as for the parameters considered in the simulations herd immunity is not reached before eradication under constant testing. Whether eradication or containment strategies should be preferred depends on considerations about testing availability, possible long-term effects of infections on the health of individuals [Davis et al., 2020] and the impact of the epidemic on the economy, and is outside of the scope of this work. Our objective here was to derive the optimal containment strategy for cases when eradication is simply not possible, e.g., because of test scarcity or budget limitations.

Second, we derived our results for a standard SIR model (yet with extensions to testing and symptomatic individuals). Our objective was to derive analytic insights for a model of epidemics that is general enough to encode the core traits of an epidemic without getting lost in the details of specific diseases. Clearly, caution is required when applying

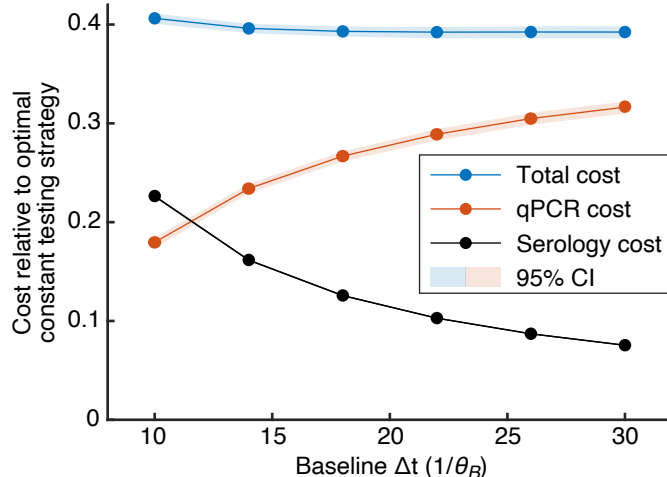


Figure 6: Cost of the optimal testing policy for the optimization problem 4, as a function of different baseline testing rates θ_B . Costs are normalized with respect to the cost of the constant testing policy with the minimum testing frequency required to maintain the constraints $I_u + I_d \leq I_{\max}$ at all times (Materials and Methods Section 4.2). Data points connected by straight lines are mean statistics across 1000 simulations of the stochastic trajectories. Shaded bands represent 95% confidence intervals. Orange and black data points report the relative contribution of adaptive qPCR testing and baseline serology testing to the total cost (blue points), respectively. All adaptive policies induce significant cost savings, up to 60% reduction with respect to the cost under the optimal constant testing strategy derived in Section 4.2 for the parameters investigated. Model parameters and initial conditions are as in the Materials and Methods Table 1 and Section 4.7.

our findings in the field and additional steps are needed to validate our suggestions with detailed models of any specific disease before translation to practice. We note especially that we did not account explicitly for delays due to test processing time in our model. However, the fact that serology has typically a faster turnaround time than qPCR is an additional argument in support of serology as a baseline testing tool.

Finally, we investigated the robustness of our procedure to sources of stochasticity that are intrinsic to the spread of an epidemic, and found that using information on the expected scaling of fluctuations with the population size and the state of the epidemic, one can apply the testing strategies developed for the deterministic SIR model to control epidemics even in the presence of intrinsic stochasticity. In practical applications, one may encounter additional sources of exogenous stochasticity due to people’s behavioral responses, changes in policies, infections coming from external sources such as neighboring states, seasonal changes, etc. We believe that a dual approach where our theoretical results are used as a guideline for formulating candidate policies that are then tested extensively with numerical approaches adopting an ensemble of models (as in [Ray et al., 2020, Viboud and Vespignani, 2019]) would be a powerful tool in the control of future pandemics.

4 Materials and Methods

4.1 Model parameters

In our numerical studies, we used model parameters that have been used in the literature to describe the spread of COVID-19. Table 1 reports the parameter values, along with the corresponding sources. Note that we decided to use low sensitivity both for molecular

and serology testing to be conservative and to account for the fact that infected agents in the initial incubation period may not be detectable.

Parameter	Value	Sources
Transmission rate (β)	0.3 d ⁻¹	[Della Rossa et al., 2020] [Gatto et al., 2020] [Bertozzi et al., 2020]
Recovery rate (γ)	1/14 d ⁻¹	[Della Rossa et al., 2020]
Rate of symptoms development (κ)	0.04 d ⁻¹	[McAloon et al., 2020] [Gatto et al., 2020]
qPCR sensitivity (η)	0.9	[Watson et al., 2020]
Serology sensitivity (current infections) (η_{BI})	0.6	[Roche, 2020], [FDA, 2020] [Public Health England, 2020]
Serology sensitivity (past infections) (η_{BR})	0.8	[Roche, 2020], [FDA, 2020] [Public Health England, 2020]
Cost of serology relative to qPCR (c^{ser})	0.4	[Haseltine, 2020a] [Haseltine, 2020b]
Maximum adaptive testing rate (θ_{\max})	2/7 d ⁻¹	[Cashore et al., 2020]

Table 1: Parameter values and corresponding sources. Our estimate for β is a compromise between different estimates reported in the literature on COVID-19. The rate of symptoms development κ was estimated as the product of the probability of becoming symptomatic, times the incubation rate.

4.2 Constant testing strategy

One possibility for controlling an epidemic with a constant testing rate is selecting a value of the testing rate θ_{const} that guarantees a basic reproduction number [Daley and Gani, 2001] smaller than unity. For the model with symptomatic agents (Supplementary Materials Eq. S4) the basic reproduction number is

$$R_0 = \frac{\beta}{\gamma + \kappa + \eta\theta_{const}},$$

corresponding to the number of secondary infections generated by an individual when he/she is free to circulate and the rest of the population is made entirely of susceptible individuals. Setting the basic reproduction number to unity and solving for θ_{const} leads to a testing rate guaranteeing that the number of infected undetected is monotonically decreasing. This is a more restrictive condition than what is needed to satisfy the constraint $i_u + i_d \leq i_{\max}$ in Problem (4). Indeed, a lower testing rate for which the fraction of infected-undetected initially increases but reaches the constraint i_{\max} tangentially would suffice. To be fair in the comparison with the adaptive testing policy, we next derive such lower constant testing rate as a function of the fractions s_0 and i_0 of susceptible and infected individuals (all assumed to be undetected) at time $t = 0$. Note that to satisfy the constraint with the least amount of constant testing, θ_{const} should be such that $i = i_u + i_d$ reaches the constraint i_{\max} tangentially (i.e., only once at time \bar{t} with first derivative equal to zero). Our objective is to derive a series of relations between the initial state $(s(0), i_u(0), i_d(0))$, the state at time \bar{t} (i.e., $s(\bar{t}), i_u(\bar{t}), i_d(\bar{t})$), and the testing rate θ_{const} . We then exploit these relations to solve for θ_{const} . From the discussion above we have

$$i_u(\bar{t}) + i_d(\bar{t}) = i_{\max} \quad (5)$$

and

$$\frac{di(\bar{t})}{dt} = \beta s(\bar{t})i_u(\bar{t}) - \gamma i(\bar{t}) = \beta s(\bar{t})i_u(\bar{t}) - \gamma i_{\max} = 0. \quad (6)$$

Next, by Eq. (1) it holds $ds(t)/dt = -\beta s(t)i_u(t)$ and $di_d(t)/dt + dr(t)/dt = (\eta\theta_{const} + \gamma)i_u(t)$ leading to

$$\frac{1}{s(t)} \frac{ds(t)}{dt} + \frac{\beta}{(\eta\theta_{const} + \gamma)} \frac{d(i_d(t) + r(t))}{dt} = 0.$$

Integrating this equation we can derive a constant of motion for the epidemic which leads to the following relation between the epidemic state at time zero and at time \bar{t} :

$$\ln\left(\frac{s(\bar{t})}{s_0}\right) - \frac{\beta}{\gamma + \eta\theta_{const}} (s(\bar{t}) + i_u(\bar{t}) - s_0 - i_0) = 0. \quad (7)$$

Finally, integrating $di_d(t)/dt = \eta\theta_{const}i_u(t) - \gamma i_d(t)$ in the interval $[0, \bar{t}]$ we obtain

$$i_d(\bar{t}) = \eta\theta_{const} e^{-\gamma\Delta t(s(\bar{t}), s_0, i_0)} \int_{s(\bar{t})}^{s_0} \frac{e^{\gamma\Delta t(s, s_0, i_0)}}{\beta s} ds = i_{\max} - i_u(\bar{t}), \quad (8)$$

where we used $i_d(0) = 0$ and a reformulation $\Delta t(\bar{s}, s_0, i_0)$ of the time interval such that $s(\Delta t) = \bar{s}$ as a function of the epidemic state as introduced in [Harko et al., 2014] and detailed in Supplementary Materials Eq. (S6). Solving Eqs. (5)-(8) for the unknowns $s(\bar{t}), i_u(\bar{t}), i_d(\bar{t}), \theta_{const}$ leads to the minimum constant testing rate θ_{const} that ensures $i(t) = i_u(t) + i_d(t) \leq i_{\max}$ for all t .

4.3 Observability notions

We formally define observability for a parametric system as follows.

Definition 1. A dynamical system $dx(t)/dt = g(x(t), \beta(t))$ with state $x(t)$ and time-varying parameter $\beta(t)$ is observable from the output $y(t) = h(x(t))$ if for any two observed outputs $y_1(t)$ and $y_2(t)$, the condition $y_1(t) \equiv y_2(t)$ for all t implies $x_1(0) = x_2(0)$ and $\beta_1(t) \equiv \beta_2(t)$ for all t .

Lemma 1 (Observability from molecular testing). Consider the system of Eq. (1) with state $x(t) = [s(t), i_u(t), i_d(t), r(t)]$ and continuous time output $y(t) = i_d(t)$. Suppose that $\eta\theta(t) > 0$ for all t and that γ is known.

1. If $\beta(t) \equiv \beta$, the system is observable.
2. If $\beta(t)$ is time-varying, the system is not observable.

Lemma 2 (Observability from serology testing). Consider the system of Eq. (3) with state $x(t) = [s(t), i_u(t), i_d(t), r_u(t), r_d(t)]$ and continuous time output $y(t) = [i_d(t), r_d(t)]$. If $\eta\theta(t) + \eta_{BR}\theta_B > 0$ and γ is known, the system is observable.

The proofs of these lemmas are provided in the Supplementary Materials.

4.4 Stochastic model

We performed stochastic simulations of a compartmental model of epidemics in which individuals of a population of size N are assigned to the same compartments S, I_u, I_d, R_u and R_d as in the deterministic SIR model with symptomatic individuals (Supplementary

Materials Eq. (S4)). In analogy with the deterministic SIR model, transition rates among states are set to:

$$\begin{aligned}
W(S-1, I_u+1, I_d, R_u | S, I_u, I_d, R_u) &= \beta \frac{SI_u}{N} && \text{(new infection)} \\
W(S, I_u-1, I_d, R_u+1 | S, I_u, I_d, R_u) &= \gamma I_u && \text{(recovery of } I_u) \\
W(S, I_u-1, I_d+1, R_u | S, I_u, I_d, R_u) &= [\eta\theta + \kappa + \theta_B \eta_{BI}] I_u && \text{(detection of } I_u) \\
W(S, I_u, I_d-1, R_u | S, I_u, I_d, R_u) &= \gamma I_d && \text{(recovery of } I_d) \\
W(S, I_u, I_d, R_u-1 | S, I_u, I_d, R_u) &= \theta_B \eta_{BR} R_u && \text{(detection of } R_u)
\end{aligned}$$

where $W(X'|X)$ is the probability per unit time of transitioning from state X to state X' and the parameters have the same interpretation as in the deterministic SIR model, and capital letters S , I_u , I_d and R_u indicate the absolute number of individuals in the various compartments of the stochastic model. The compartment R_d is not mentioned explicitly, as its abundance is equal to $N - S - I_u - I_d - R_u$. Unlike the deterministic SIR model, the stochastic model of epidemics accounts for the fact that the numbers of individuals in each compartment are integers and that infection, recovery and detection are stochastic events. As such, the stochastic model is better suited to describing epidemics in small populations or the epidemiological dynamics in the initial phases of an epidemic, where number fluctuations can be important. The dynamics of the stochastic model is governed by the master equation, [van Kampen, 2007, Gardiner, 2009]:

$$\begin{aligned}
\frac{\partial P}{\partial t}(S, I_u, I_d, R_u, t) &= \left((\mathbf{E}_S^{+1} \mathbf{E}_{I_u}^{-1} - 1) \beta \frac{SI_u}{N} + (\mathbf{E}_{I_u}^{+1} \mathbf{E}_{R_u}^{-1} - 1) \gamma I_u + \right. \\
&\quad + \left(\mathbf{E}_{I_u}^{+1} \mathbf{E}_{I_d}^{-1} - 1 \right) I_u (\eta\theta + \kappa + \theta_B \eta_{BI}) + \left(\mathbf{E}_{I_d}^{+1} - 1 \right) \gamma I_d + \\
&\quad \left. + (\mathbf{E}_{R_u}^{+1} - 1) \theta_B \eta_{BR} R_u \right) P(S, I_u, I_d, R_u, t), \tag{9}
\end{aligned}$$

where $P(S, I_u, I_d, R_u, t)$ is the probability of being in state $X := [S, I_u, I_d, R]$ at time t and the transition operator $\mathbf{E}_S^{\pm 1}$ is defined by $\mathbf{E}_S^{\pm 1} f(S, I_u, I_d, R_u) = f(S \pm 1, I_u, I_d, R_u)$ for a generic function f , and similarly for the other operators.¹ We simulated trajectories of the stochastic model of epidemics by using the Gillespie algorithm [Gillespie, 1976], with the parameters reported in Table 1.

For large N , Eq. (9) can be expanded in powers of $1/N$ following a Kramers-Moyal or system-size expansion [van Kampen, 2007, Gardiner, 2009]. Eq. (9) can be expressed in terms of the rescaled variables $\tilde{x} := X/N = [\tilde{s}, \tilde{i}_u, \tilde{i}_d, \tilde{r}_u]$ as follows:

$$\begin{aligned}
\frac{1}{N} \frac{\partial p}{\partial t}(\tilde{s}, \tilde{i}_u, \tilde{i}_d, \tilde{r}_u, t) &= \left(\left(\mathbf{E}_{\tilde{s}}^{+\frac{1}{N}} \mathbf{E}_{\tilde{i}_u}^{-\frac{1}{N}} - 1 \right) \beta \tilde{s} \tilde{i}_u + \left(\mathbf{E}_{\tilde{i}_u}^{+\frac{1}{N}} \mathbf{E}_{\tilde{r}_u}^{-\frac{1}{N}} - 1 \right) \gamma \tilde{i}_u + \right. \\
&\quad + \left(\mathbf{E}_{\tilde{i}_u}^{+\frac{1}{N}} \mathbf{E}_{\tilde{i}_d}^{-\frac{1}{N}} - 1 \right) \tilde{i}_u (\eta\theta + \kappa + \theta_B \eta_{BI}) + \left(\mathbf{E}_{\tilde{i}_d}^{+\frac{1}{N}} - 1 \right) \gamma \tilde{i}_d + \\
&\quad \left. + \left(\mathbf{E}_{\tilde{r}_u}^{+\frac{1}{N}} - 1 \right) \theta_B \eta_{BR} \tilde{r}_u \right) p(\tilde{s}, \tilde{i}_u, \tilde{i}_d, \tilde{r}_u, t). \tag{10}
\end{aligned}$$

Note that $\tilde{x}(t)$ is a stochastic process, whereas $x(t)$ as defined in the main text is the solution to the deterministic SIR model. The right hand side of Eq. (10) is a function of $\tilde{x} \pm 1/N$. Expanding this function around \tilde{x} up to the second order ($1/N^2$), one obtains

¹In Eq. (9), operators within parentheses act on all the functions of state variables to their right according to conventional operator precedence, e.g. $(\mathbf{E}_S^{+1} \mathbf{E}_{I_u}^{-1} - 1) SI_u P(S, I_u, I_d, R_u, t)$ is to be interpreted as $(\mathbf{E}_S^{+1} \mathbf{E}_{I_u}^{-1} - 1) SI_u P(S, I_u, I_d, R_u, t) = \mathbf{E}_S^{+1} \mathbf{E}_{I_u}^{-1} (SI_u P(S, I_u, I_d, R_u, t)) - SI_u P(S, I_u, I_d, R_u, t) = (S+1)(I_u-1)P(S+1, I_u-1, I_d, R_u, t) - SI_u P(S, I_u, I_d, R_u, t)$.

the Fokker-Planck equation:

$$\frac{\partial p}{\partial t}(\tilde{x}, t) = - \sum_j \frac{\partial}{\partial \tilde{x}_j} (g_j(\tilde{x}, \theta) p(\tilde{x}, t)) + \frac{1}{2N} \sum_{j,k} \frac{\partial^2}{\partial \tilde{x}_j \partial \tilde{x}_k} (B_{jk}(\tilde{x}, \theta) p(\tilde{x}, t)), \quad (11)$$

where g is the vector field corresponding to the deterministic dynamics used for computing the optimal testing strategy (see Eq. (4) and Eq. (S4) in the Supplementary Materials) and B is the matrix:

$$B(\tilde{x}, \theta) = \begin{bmatrix} \beta \tilde{s} \tilde{i}_u & -\beta \tilde{s} \tilde{i}_u & 0 & 0 \\ -\beta \tilde{s} \tilde{i}_u & [\beta \tilde{s} + \gamma + \eta \theta + \kappa + \theta_B \eta_{BI}] \tilde{i}_u & -[\eta \theta + \kappa + \theta_B \eta_{BI}] \tilde{i}_u & -\gamma \tilde{i}_u \\ 0 & -[\eta \theta + \kappa + \theta_B \eta_{BI}] \tilde{i}_u & [\eta \theta + \kappa + \theta_B \eta_{BI}] \tilde{i}_u + \gamma \tilde{i}_d & 0 \\ 0 & -\gamma \tilde{i}_u & 0 & \gamma \tilde{i}_u + \theta_B \eta_{BR} \tilde{r}_u \end{bmatrix}.$$

Eq. (11) is known as the diffusion approximation of the master Eq. (10) and describes the probability distribution of a continuous stochastic process specified by the following Itô Langevin equation: [van Kampen, 2007, Gardiner, 2009]

$$\frac{d\tilde{x}}{dt} = g(\tilde{x}, \theta) + \frac{1}{\sqrt{N}} \varepsilon(\tilde{x}, \theta, t), \quad (12)$$

where $\varepsilon(\tilde{x}, \theta, t)$ is a Gaussian noise with covariance $\langle \varepsilon_j(\tilde{x}(t), \theta(t), t) \varepsilon_k(\tilde{x}(t'), \theta(t'), t') \rangle = B_{jk}(\tilde{x}(t), \theta(t)) \delta(t - t')$ and zero mean, where δ is the Dirac delta. Intuitively, in Eq. (12) the first term $g(\tilde{x}, \theta)$ coincides with the vector field of the deterministic dynamics while the second term captures diffusive fluctuations due to stochasticity, whose amplitude depends both on the population size and on the epidemic state. As detailed in the next section, this approach enables us to characterize the process noise for the extended Kalman filter with the correct scaling in N and highlights its dependence on the current epidemic state (e.g., the number of infected-undetected) as captured by the matrix B .

4.5 State estimation for the stochastic simulations

Given the dynamics of Eq. (12), we discuss here how we estimate the state of the epidemic. We assume the following observation model:

$$\tilde{y}(t_k) = [\tilde{i}_d(t_k); \tilde{r}_d(t_k)] = C \tilde{x}(t_k) + c \quad (13)$$

with:

$$C = \begin{bmatrix} 0 & 0 & 0 & 1 \\ -1 & -1 & -1 & -1 \end{bmatrix}, \quad c = \begin{bmatrix} 0 \\ q \end{bmatrix},$$

that is, only infected-detected and recovered-detected are observed, and we assume discrete observation times t_k (e.g., daily observations). Such observations can be used to estimate the state of the system via a state observer, which we implemented using an extended Kalman filter with state constraints (see [King et al., 2008, Pasetto et al., 2017, Pasetto et al., 2018, Li et al., 2020b] for other applications of the Kalman filter in the context of epidemiology).

In a Kalman filter, observations $y_k = \tilde{y}(t_k)$ are used to create an estimate of the state, denoted by $\hat{x}(t) = [\hat{s}(t); \hat{i}_u(t); \hat{i}_d(t); \hat{r}_u(t)]$. The first step is to initialize $\hat{x}_{0|0} = \mathbb{E}[x(t_0)]$, $P_{0|0} = \mathbb{E}[(x(t_0) - \hat{x}(t_0))(x(t_0) - \hat{x}(t_0))^\top]$. Then, the dynamics of the extended Kalman filter [Khalil, 2015] is computed as follows, at any time step t_k :

1. Predict the next state, given previous observations:

$$\begin{cases} \frac{d\hat{x}(t)}{dt} = g(\hat{x}(t), \theta(t)) \\ \frac{dP(t)}{dt} = G(t)P(t) + P(t)G(t)^\top + Q(t) \end{cases} \quad \text{with} \quad \begin{cases} \hat{x}(t_k) = \hat{x}_{k|k} \\ P(t_k) = P_{k|k} \end{cases} \quad \text{and} \quad G(t) = \left. \frac{\partial g}{\partial x} \right|_{\hat{x}(t), \theta(t)}$$

and set $\hat{x}_{k+1|k} = \hat{x}(t_{k+1})$, $P_{k+1|k} = P(t_k)$

2. Update the prediction, given the current observation:

$$\begin{aligned} K_{k+1} &= P_{k+1|k} C^\top (C P_{k+1|k} C^\top + R)^{-1} \\ \hat{x}_{k+1|k+1} &= \Pi_{X_{k+1}} [\hat{x}_{k+1|k} + K_{k+1} (y_{k+1} - C \hat{x}_{k+1|k})] \\ P_{k+1|k+1} &= (I - K_{k+1} C) P_{k+1|k}, \end{aligned}$$

where Π_{X_k} represents the projection in the feasible set $X_k = \{x \geq 0 \mid Cx + c = y_k\}$.

The matrices Q and R are covariance matrices for the process and measurement noise. In our analysis, we assume $R = 0$ (as the number of infected-detected and recovered-detected is perfectly known by the policy maker and thus there is no measurement error in Eq. (13)), while $Q(t)$ is the covariance of the process noise, which is equal to B/N as derived from the expansion of the master equation in Section 4.4.

4.6 Testing strategy for the stochastic simulations

The testing policy derived for the deterministic SIR model is not necessarily robust to the presence of stochastic fluctuations. For this reason, in the stochastic simulations we implemented a receding horizon version $\hat{\theta}^*(t)$ of the testing policy where at any time $t_k > t_A$ (as defined in Fig. 4) we computed the constant testing rate needed to drive the total fraction of infected to the threshold i_{\max} in a horizon of H days (we set $H = 3$ d), assuming that the dynamics follows the deterministic SIR model, i.e. Eq. (S4) in the Supplementary Materials. According to the principles of receding horizon control, such testing rate is applied for one time step and then a new problem is solved for the next horizon $[t_{k+1}, t_{k+1} + H]$ given the new realized state. Thus, at every time step t_k the testing rate is set to:

$$\hat{\theta}^*(t_k) = \begin{cases} 0 & \text{if } t_k < t_A \\ \max(\{0, \min\{\theta_{\max}, \theta_{rh}(\hat{s}(t_k), \hat{i}_u(t_k))\}\}) & \text{otherwise} \end{cases} \quad (14)$$

where θ_{rh} is the testing rate that would bring the deterministic system to the constraint $\hat{i}_u + \hat{i}_d = i_{\max}$ with zero derivative in a time horizon H , starting from $\hat{s}(t_k)$ and $\hat{i}_u(t_k)$ (see Eq. (S16) in the Supplementary Materials). Note that we assume here that the receding horizon is implemented for any time $t_k > t_A$, where t_A is the optimal time to start testing as computed for the deterministic SIR model. In practice, the policy maker may prefer to implement the receding horizon control from the beginning, for additional robustness and to compensate for the uncertainty of state estimates in the early phases of the dynamics. This has a minor cost implications, since t_A is typically very small with the parameters considered here.

4.7 Parameters used in simulations of the stochastic model of epidemics

Simulations of the stochastic model of epidemics were performed with population size $N = 50000$ and constraint $I_{\max} = 1000$ corresponding to 2% of the population size. This percentage was chosen for illustration purposes and it roughly corresponds to the peak percentage quarantine capacity estimated to be required for the safe reopening of Cornell's Ithaca NY campus during the COVID-19 pandemic in the Fall 2020 [Cashore et al., 2020]. Realizations of stochastic epidemics were initialized with $I(0) = I_u(0) = 50$ infected and $S(0) = N - 50$ susceptible individuals (the other compartments were initialized at $I_d(0) = R_d(0) = R_u(0) = 0$). The other parameters were set to the values in Table 1. The initial state estimate for the extended Kalman filter was set to $\hat{I}(0) = 0$ infected and

$\hat{S}(0) = N$ susceptible individuals (the estimates for the other compartments were set to zero). All entries of the initial estimate for the covariance matrix P (see Section 4.5) of the extended Kalman filter were set to zero, with the exception of the estimate for the variance of $\hat{S}(0)$ and of $\hat{I}_u(0)$, which were set to $I_{\max}^2/12$, to reflect a large uncertainty on the initial condition.

References

- [AACC, 2020] AACC (2020). Coronavirus testing survey. Technical report, American Association for Clinical Chemistry. <https://www.aacc.org/science-and-research/covid-19-resources/aacc-covid-19-testing-survey>.
- [Acemoglu et al., 2020a] Acemoglu, D., Chernozhukov, V., Werning, I., and Whinston, M. D. (2020a). Optimal Targeted Lockdowns in a Multi-Group SIR Model. Working Paper 27102, National Bureau of Economic Research.
- [Acemoglu et al., 2020b] Acemoglu, D., Makhdoumi, A., Malekian, A., and Ozdaglar, A. E. (2020b). Testing, Voluntary Social Distancing and the Spread of an Infection. Working Paper 27483, National Bureau of Economic Research.
- [Alvarez et al., 2020] Alvarez, F. E., Argente, D., and Lippi, F. (2020). A simple planning problem for covid-19 lockdown. Working Paper 26981, National Bureau of Economic Research.
- [Anderson and May, 1992] Anderson, R. M. and May, R. M. (1992). *Infectious Diseases of Humans: Dynamics and Control*. Oxford university press.
- [Andersson and Britton, 2012] Andersson, H. and Britton, T. (2012). *Stochastic Epidemic Models and Their Statistical Analysis*, volume 151. Springer Science & Business Media.
- [Apuzzo and Gebredikan, 2020] Apuzzo, M. and Gebredikan, S. (2020). Can’t Get Tested? Maybe You’re in the Wrong Country. *The New York Times*, March 20, 2020.
- [Atkeson, 2020] Atkeson, A. (2020). What Will Be the Economic Impact of COVID-19 in the US? Rough Estimates of Disease Scenarios. Working Paper 26867, National Bureau of Economic Research.
- [Beal et al., 2018] Beal, L., Hill, D., Martin, R., and Hedengren, J. (2018). GEKKO Optimization Suite. *Processes*, 6(8):106.
- [Behncke, 2000] Behncke, H. (2000). Optimal control of deterministic epidemics. *Optimal control applications and methods*, 21(6):269–285.
- [Berger et al., 2020] Berger, D. W., Herkenhoff, K. F., and Mongey, S. (2020). An seir infectious disease model with testing and conditional quarantine. Working Paper 26901, National Bureau of Economic Research.
- [Bertozzi et al., 2020] Bertozzi, A. L., Franco, E., Mohler, G., Short, M. B., and Sledge, D. (2020). The challenges of modeling and forecasting the spread of COVID-19. *Proceedings of the National Academy of Sciences*, 117(29):16732–16738.
- [Bertuzzo et al., 2020] Bertuzzo, E., Mari, L., Pasetto, D., Miccoli, S., Casagrandi, R., Gatto, M., and Rinaldo, A. (2020). The geography of COVID-19 spread in Italy and implications for the relaxation of confinement measures. *Nature Communications*, 11(4264).

- [Brotherhood et al., 2020] Brotherhood, L., Kircher, P., Santos, C., and Tertilt, M. (2020). An Economic Model of the Covid-19 Epidemic: The Importance of Testing and Age-Specific Policies. CESifo Working Paper Series 8316, CESifo.
- [Cashore et al., 2020] Cashore, J., Duan, N., Janmohamed, A., Wan, J., Zhang, Y., Henderson, S., Shmoys, D., and Frazier, P. (2020). COVID-19 Mathematical Modeling for Cornell’s Fall Semester. Technical report, Cornell University.
- [Chinazzi et al., 2020] Chinazzi, M., Davis, J. T., Ajelli, M., Gioannini, C., Litvinova, M., Merler, S., y Piontti, A. P., Mu, K., Rossi, L., Sun, K., et al. (2020). The effect of travel restrictions on the spread of the 2019 novel coronavirus (COVID-19) outbreak. *Science*, 368(6489):395–400.
- [Chu et al., 2020] Chu, D. K., Akl, E. A., Duda, S., Solo, K., Yaacoub, S., Schünemann, H. J., El-harakeh, A., Bognanni, A., Lotfi, T., Loeb, M., et al. (2020). Physical distancing, face masks, and eye protection to prevent person-to-person transmission of SARS-CoV-2 and COVID-19: a systematic review and meta-analysis. *The Lancet*, 395(10242).
- [Daley and Gani, 2001] Daley, D. J. and Gani, J. (2001). *Epidemic Modelling: An Introduction*. Cambridge University Press.
- [Davis et al., 2020] Davis, H. E., Assaf, G. S., McCorkell, L., Wei, H., Low, R. J., Re’em, Y., Redfield, S., Austin, J. P., and Akrami, A. (2020). Characterizing long covid in an international cohort: 7 months of symptoms and their impact. *medRxiv*, 2020.12.24.20248802.
- [Della Rossa et al., 2020] Della Rossa, F., Salzano, D., Di Meglio, A., De Lellis, F., Coraggio, M., Calabrese, C., Guarino, A., Cardona-Rivera, R., De Lellis, P., Liuzza, D., et al. (2020). A network model of Italy shows that intermittent regional strategies can alleviate the COVID-19 epidemic. *Nature communications*, 11(1):1–9.
- [Di et al., 2020] Di, L. D., Pullano, G., Sabbatini, C., Boëlle, P., and Colizza, V. (2020). Impact of lockdown on COVID-19 epidemic in Île-de-France and possible exit strategies. *BMC medicine*, 18(1):240–240.
- [Di Giamberardino and Iacoviello, 2017] Di Giamberardino, P. and Iacoviello, D. (2017). Optimal control of SIR epidemic model with state dependent switching cost index. *Biomedical Signal Processing and Control*, 31:377–380.
- [Diekmann and Heesterbeek, 2000] Diekmann, O. and Heesterbeek, J. (2000). *Mathematical Epidemiology of Infectious Diseases: Model Building, Analysis and Interpretation*. John Wiley.
- [Drakopoulos and Randhawa, 2020] Drakopoulos, K. and Randhawa, R. S. (2020). Why perfect tests may not be worth waiting for: Information as a commodity. Available at SSRN: <https://ssrn.com/abstract=3565245>.
- [Farboodi et al., 2020] Farboodi, M., Jarosch, G., and Shimer, R. (2020). Internal and external effects of social distancing in a pandemic. Working Paper 27059, National Bureau of Economic Research.
- [FDA, 2020] FDA (2020). Independent Evaluations of COVID-19 Serological Tests. Technical report, U.S. Department of Health and Human Services Food and Drug Administration.

- [Fink and Baker, 2020] Fink, S. and Baker, M. (2020). ‘It’s Just Everywhere Already’: How Delays in Testing Set Back the U.S. Coronavirus Response. *The New York Times*, March 10, 2020.
- [Flaxman et al., 2020] Flaxman, S., Mishra, S., Gandy, A., Unwin, H. J. T., Mellan, T. A., Coupland, H., Whittaker, C., Zhu, H., Berah, T., Eaton, J. W., et al. (2020). Estimating the effects of non-pharmaceutical interventions on COVID-19 in Europe. *Nature*, 584(7820):257–261.
- [Gardiner, 2009] Gardiner, C. (2009). *Stochastic Methods: A Handbook for the Natural and Social Sciences*. Springer Series in Synergetics. Springer Berlin Heidelberg.
- [Gatto et al., 2020] Gatto, M., Bertuzzo, E., Mari, L., Miccoli, S., Carraro, L., Casagrandi, R., and Rinaldo, A. (2020). Spread and dynamics of the COVID-19 epidemic in Italy: Effects of emergency containment measures. *Proceedings of the National Academy of Sciences*, 117(19):10484–10491.
- [Gillespie, 1976] Gillespie, D. T. (1976). A general method for numerically simulating the stochastic time evolution of coupled chemical reactions. *Journal of Computational Physics*, 22(4):403–434.
- [Gollier and Gossner, 2020] Gollier, C. and Gossner, O. (2020). Group testing against Covid-19. *Covid Economics*, 1(2):32–42.
- [Grassly et al., 2020] Grassly, N., Pons, S. M., Parker, E., White, P., Ainslie, K., Baguelin, M., Bhatt, S., Boonyasiri, A., Boyd, O., Brazeau, N., Cattarino, L., Ciavarella, C., Cooper, L., Coupland, H., Cucunuba, P. Z., Cuomo-Dannenburg, G., Dighe, A., Djaa-fara, A., Donnelly, C., Dorigatti, I., van, E. S., Ferreira, D. N. F., Fitzjohn, R., Fu, H., Gaythorpe, K., Geidelberg, L., Green, W., Hallett, T., Hamlet, A., Hayes, S., Hinsley, W., Imai, N., Jorgensen, D., Knock, E., Laydon, D., Lees, J., Mangal, T., Mellan, T., Mishra, S., Nedjati, G. G., Nouvellet, P., Okell, L., Ower, A., Parag, K., Pickles, M., Ragonnet-Cronin, M., Stopard, I., Thompson, H., Unwin, H., Verity, R., Vollmer, M., Volz, E., Walker, P., Walters, C., Wang, H., Wang, Y., Watson, O., Whittaker, C., Whittles, L., Winskill, P., Xi, X., and Ferguson, N. (2020). Report 16: Role of testing in COVID-19 control. Technical report, Imperial College London.
- [Harko et al., 2014] Harko, T., Lobo, F. S., and Mak, M. (2014). Exact analytical solutions of the Susceptible-Infected-Recovered (SIR) epidemic model and of the SIR model with equal death and birth rates. *Applied Mathematics and Computation*, 236:184 – 194.
- [Haseltine, 2020a] Haseltine, W. (2020a). How Antibody Tests Can Be Used To Fight COVID-19. *Forbes*, April 6, 2020.
- [Haseltine, 2020b] Haseltine, W. (2020b). Tests For COVID-19 Are Expensive, But They Don’t Have To Be. *Forbes*, April 8, 2020.
- [Hota and Gupta, 2020] Hota, A. R. and Gupta, K. (2020). A generalized SIS epidemic model on temporal networks with asymptomatic carriers and comments on decay ratio. *arXiv preprint arXiv:2008.00826*.
- [Hota and Sundaram, 2019] Hota, A. R. and Sundaram, S. (2019). Game-theoretic vaccination against networked SIS epidemics and impacts of human decision-making. *IEEE Transactions on Control of Network Systems*, 6(4):1461–1472.
- [Keeling and Rohani, 2011] Keeling, M. J. and Rohani, P. (2011). *Modeling Infectious Diseases in Humans and Animals*. Princeton University Press.

- [Kermack and McKendrick, 1927] Kermack, W. O. and McKendrick, A. G. (1927). A contribution to the mathematical theory of epidemics. *Proceedings of the Royal Society of London. Series A, Containing Papers of a Mathematical and Physical Character*, 115(772):700–721.
- [Khalil, 2015] Khalil, H. K. (2015). *Nonlinear control*. Pearson.
- [King et al., 2008] King, A. A., Ionides, E. L., Pascual, M., and Bouma, M. J. (2008). Inapparent infections and cholera dynamics. *Nature*, 454(7206):877–880.
- [Kraay et al., 2020] Kraay, A. N., Nelson, K. N., Zhao, C. Y., Weitz, J. S., and Lopman, B. A. (2020). Modeling serological testing to inform relaxation of social distancing for COVID-19 control. *medRxiv*, 2020.04.24.20078576.
- [Kruse and Strack, 2020] Kruse, T. and Strack, P. (2020). Optimal control of an epidemic through social distancing. *Cowles Foundation Discussion Paper No. 2229, Available at SSRN: <https://ssrn.com/abstract=3583186>*.
- [Kubina and Dziedzic, 2020] Kubina, R. and Dziedzic, A. (2020). Molecular and serological tests for COVID-19 a comparative review of SARS-CoV-2 coronavirus laboratory and point-of-care diagnostics. *Diagnostics*, 10(6):434.
- [Kucirka et al., 2020] Kucirka, L. M., Lauer, S. A., Laeyendecker, O., Boon, D., and Lessler, J. (2020). Variation in false-negative rate of reverse transcriptase polymerase chain reaction–based SARS-CoV-2 tests by time since exposure. *Annals of Internal Medicine*.
- [Larremore et al., 2020] Larremore, D. B., Wilder, B., Lester, E., Shehata, S., Burke, J. M., Hay, J. A., Tambe, M., Mina, M. J., and Parker, R. (2020). Test sensitivity is secondary to frequency and turnaround time for COVID-19 screening. *Science Advances*, eabd5393.
- [Li et al., 2020a] Li, G., Shivam, S., Hochberg, M. E., Wardi, Y., and Weitz, J. S. (2020a). Disease-dependent interaction policies to support health and economic outcomes during the COVID-19 epidemic. *medRxiv 2020.08.24.20180752*.
- [Li et al., 2020b] Li, R., Pei, S., Chen, B., Song, Y., Zhang, T., Yang, W., and Shaman, J. (2020b). Substantial undocumented infection facilitates the rapid dissemination of novel coronavirus (SARS-CoV-2). *Science*, 368(6490):489–493.
- [McAloon et al., 2020] McAloon, C., Collins, Á., Hunt, K., Barber, A., Byrne, A. W., Butler, F., Casey, M., Griffin, J., Lane, E., McEvoy, D., Wall, P., Green, M., O’Grady, L., and More, S. J. (2020). Incubation period of COVID-19: a rapid systematic review and meta-analysis of observational research. *BMJ Open*, 10(8).
- [Mervosh and Fernandez, 2020] Mervosh, S. and Fernandez, M. (2020). Months Into Virus Crisis, U.S. Cities Still Lack Testing Capacity. *The New York Times*, July 6, 2020.
- [Miclo et al., 2020] Miclo, L., Spiro, D., and Weibull, J. (2020). Optimal epidemic suppression under an ICU constraint. *arXiv preprint arXiv:2005.01327*.
- [Nowzari et al., 2016] Nowzari, C., Preciado, V. M., and Pappas, G. J. (2016). Analysis and control of epidemics: A survey of spreading processes on complex networks. *IEEE Control Systems Magazine*, 36(1):26–46.
- [OECD, 2020] OECD (2020). Testing for COVID-19: A way to lift confinement restrictions. Technical report, Organisation for Economic Co-operation and Development.

- [Paré et al., 2017] Paré, P. E., Beck, C. L., and Nedić, A. (2017). Epidemic processes over time-varying networks. *IEEE Transactions on Control of Network Systems*, 5(3):1322–1334.
- [Paré et al., 2020] Paré, P. E., Liu, J., Beck, C. L., Kirwan, B. E., and Başar, T. (2020). Analysis, Estimation, and Validation of Discrete-Time Epidemic Processes. *IEEE Transactions on Control Systems Technology*, 28(1):79–93.
- [Pasetto et al., 2018] Pasetto, D., Finger, F., Camacho, A., Grandesso, F., Cohuet, S., Lemaitre, J. C., Azman, A. S., Luquero, F. J., Bertuzzo, E., and Rinaldo, A. (2018). Near real-time forecasting for cholera decision making in Haiti after Hurricane Matthew. *PLoS computational biology*, 14(5):e1006127.
- [Pasetto et al., 2017] Pasetto, D., Finger, F., Rinaldo, A., and Bertuzzo, E. (2017). Real-time projections of cholera outbreaks through data assimilation and rainfall forecasting. *Advances in Water Resources*, 108:345–356.
- [Pastor-Satorras et al., 2015] Pastor-Satorras, R., Castellano, C., Van Mieghem, P., and Vespignani, A. (2015). Epidemic processes in complex networks. *Reviews of modern physics*, 87(3):925.
- [Public Health England, 2020] Public Health England (2020). Evaluation of Roche Elecsys AntiSARS-CoV-2 serology assay for the detection of anti-SARS-CoV-2 antibodies. Technical report, Public Health England.
- [Pullano et al., 2020] Pullano, G., Di Domenico, L., Sabbatini, C. E., Valdano, E., Turbelin, C., Debin, M., Guerrisi, C., Kengne-Kuetché, C., Souty, C., Hanslik, T., Blanchon, T., Boëlle, P.-Y., Figoni, J., S, V., Campèse, C., Bernard-Stoecklin, S., and Colizza, V. (2020). Underdetection of COVID-19 cases in France threatens epidemic control. *Nature*, Online ahead of print.
- [Ray et al., 2020] Ray, E. L., Wattanachit, N., Niemi, J., Kanji, A. H., House, K., Cramer, E. Y., Bracher, J., Zheng, A., Yamana, T. K., Xiong, X., Woody, S., Wang, Y., Wang, L., Walraven, R. L., Tomar, V., Sherratt, K., Sheldon, D., Reiner, R. C., Prakash, B. A., Osthus, D., Li, M. L., Lee, E. C., Koyluoglu, U., Keskinocak, P., Gu, Y., Gu, Q., George, G. E., España, G., Corsetti, S., Chhatwal, J., Cavany, S., Biegel, H., Ben-Nun, M., Walker, J., Slayton, R., Lopez, V., Biggerstaff, M., Johansson, M. A., and Reich, N. G. (2020). Ensemble Forecasts of Coronavirus Disease 2019 (COVID-19) in the U.S. *medRxiv*, 2020.08.19.20177493.
- [Roche, 2020] Roche (2020). Elecsys®Anti-SARS-CoV-2. Package Insert 2020-07, V4.0; Material Numbers 09203095190 and 09203079190.
- [Sharma and Samanta, 2015] Sharma, S. and Samanta, G. (2015). Stability analysis and optimal control of an epidemic model with vaccination. *International Journal of Biomathematics*, 8(03):1550030.
- [Spence and Starrett, 1975] Spence, M. and Starrett, D. (1975). Most rapid approach paths in accumulation problems. *International Economic Review*, 16(2):388–403.
- [Stock, 2020] Stock, J. H. (2020). Data gaps and the policy response to the novel coronavirus. Working Paper 26902, National Bureau of Economic Research.
- [van Kampen, 2007] van Kampen, N. (2007). *Stochastic Processes in Physics and Chemistry*. North-Holland Personal Library. Elsevier, Amsterdam, third edition.

- [Vespignani et al., 2020] Vespignani, A., Tian, H., Dye, C., Lloyd-Smith, J. O., Eggo, R. M., Shrestha, M., Scarpino, S. V., Gutierrez, B., Kraemer, M. U., Wu, J., et al. (2020). Modelling COVID-19. *Nature Reviews Physics*, 2:279–281.
- [Viboud and Vespignani, 2019] Viboud, C. and Vespignani, A. (2019). The future of influenza forecasts. *Proceedings of the National Academy of Sciences*, 116(8):2802–2804.
- [Wächter and Biegler, 2006] Wächter, A. and Biegler, L. T. (2006). On the implementation of an interior-point filter line-search algorithm for large-scale nonlinear programming. *Mathematical programming*, 106(1):25–57.
- [Watson et al., 2020] Watson, J., Whiting, P. F., and Brush, J. E. (2020). Interpreting a covid-19 test result. *BMJ*, 369.
- [Weitz et al., 2020] Weitz, J. S., Park, S. W., Eksin, C., and Dushoff, J. (2020). Awareness-driven behavior changes can shift the shape of epidemics away from peaks and toward plateaus, shoulders, and oscillations. *Proceedings of the National Academy of Sciences*, 117(51):32764–32771.
- [Zaman et al., 2008] Zaman, G., Kang, Y. H., and Jung, I. H. (2008). Stability analysis and optimal vaccination of an SIR epidemic model. *BioSystems*, 93(3):240–249.
- [Zhang et al., 2020] Zhang, J., Litvinova, M., Liang, Y., Wang, Y., Wang, W., Zhao, S., Wu, Q., Merler, S., Viboud, C., Vespignani, A., Ajelli, M., and Yu, H. (2020). Changes in contact patterns shape the dynamics of the covid-19 outbreak in china. *Science*, 368(6498):1481–1486.

Supplementary Materials

S.1 Optimal testing policy

We next present the proof of the following theorem. Theorem 1 in the main text is obtained as a special case when the transmission rate is constant.

Theorem 2. *Suppose that the transmission rate $\beta(t)$ is a monotone non-increasing function of time. The optimal testing policy $\theta^\dagger(t)$ for the optimization problem of Eq. (2) with dynamics as in Eq. (1) acts in three phases:*

1. While $i_u(t) < i_{\max}$, do not test, i.e. set $\theta^\dagger(t) = 0$.
2. After $i_u(t)$ reaches i_{\max} , test with time-varying rate $\theta^\dagger(t) = (\beta(t)s(t) - \gamma)/\eta$.
3. Once herd immunity is reached, that is $s(t) = \gamma/\beta(t)$ for the first time, stop testing, i.e. set $\theta^\dagger(t) = 0$.

To prove such theorem we start with a series of auxiliary lemmas. Let t_{herd} be the first instant of time such that $s(t_{herd}) = \gamma/\beta(t_{herd})$. We say that the system reached herd immunity at time t_{herd} since for any $t > t_{herd}$ the fraction of infected naturally decreases. Mathematically,

$$\frac{di_u(t)}{dt} = (\beta(t)s(t) - \gamma)i_u(t) \leq (\beta(t_{herd})s(t_{herd}) - \gamma)i_u(t) = 0,$$

where we use the fact that in this model the susceptible and β are monotonically non-increasing. We start by proving that after herd immunity it is optimal to stop testing.

Lemma 3. *Under the optimal testing policy θ^\dagger there exists a finite time t_{herd} at which $s(t_{herd}) = \gamma/\beta(t_{herd})$. Moreover, $\theta^\dagger(t) = 0$ for all $t \geq t_{herd}$. Here the superscript \dagger denotes the evolution under the optimal testing policy.*

Proof. The fact that under the optimal testing policy herd immunity is reached is immediate as if that was not the case the objective function would be infinite. Let t_{herd} be the time when herd immunity is reached and recall that $\beta(t_{herd})s(t_{herd}) - \gamma \leq 0$ for all $t \geq t_{herd}$ since $\beta(t)$ and $s(t)$ are both decreasing with time. Consequently, $di_u(t)/dt \leq 0$ for all $t \geq t_{herd}$ and the control policy that sets $\theta^\dagger(t) = 0 \forall t \geq t_{herd}$ is feasible and therefore optimal (as no other control policy can achieve zero cost). \square

We next show that, under the optimal control, once herd immunity is reached the number of infected undetected must be at the threshold.

Lemma 4. *If the optimal objective is strictly positive, $i_u^\dagger(t_{herd}) = i_{\max}$.*

Proof. First, note that if the optimal objective is 0, this means that we do not apply any control to the system. The optimal trajectory $i_u^\dagger(t)$ is therefore at most tangent to i_{\max} , because otherwise, we would need to apply some positive control to make sure that it does not violate the constraint $i_u \leq i_{\max}$. Instead, if the optimal objective is strictly positive there is an interval of time before herd immunity is reached with positive control. If $i_u^\dagger(t_{herd}) < i_{\max}$, we could decrease the control by a small amount before reaching herd immunity (the last time the control was positive before reaching herd immunity). This would imply that i_u increase faster but for small deviations of the control we could still guarantee $i_u(t) \leq i_{\max}$ for all times. Since the rate of decrease of s increases as i_u increases, this would imply that s will decrease faster and therefore herd immunity will be reached at a time $t'_{herd} < t_{herd}$. From Lemma 3, we have that the optimal control after reaching herd immunity is identically 0. Therefore, the new control policy strictly reduces the objective, violating the optimality of the control. \square

Finally, we characterize the optimality of the proposed control θ^\dagger before t_{herd} .

Lemma 5. *The optimal control takes the most rapid approach path to reach herd immunity.*

Proof. Lemma 3 characterizes how the optimal control behaves after herd immunity. Therefore, we can rewrite the original optimization problem in Eq. (2) as follows

$$\begin{aligned} & \min \int_{t=0}^{t_{herd}} \theta(t) dt \\ \text{s.t.} \quad & i_u(t) \leq i_{\max} \quad \forall t \\ & \theta(t) \geq 0 \quad \forall t \end{aligned} \tag{S1}$$

where t_{herd} is the time to reach herd immunity (which depends on θ). Integrating the dynamics

$$\eta\theta(t) = \beta(t)s(t) - \gamma - \frac{1}{i_u(t)} \frac{di_u(t)}{dt}$$

yields

$$\begin{aligned} \eta \int_{t=0}^{t_{herd}} \theta(t) dt &= \int_{t=0}^{t_{herd}} \left(\beta s(t) - \gamma - \frac{1}{i_u(t)} \frac{di_u(t)}{dt} \right) dt \\ &= \int_{t=0}^{t_{herd}} (\beta s(t) - \gamma) dt - \int_{t=0}^{t_{herd}} \left(\frac{1}{i_u(t)} \frac{di_u(t)}{dt} \right) dt \\ &= \int_{t=0}^{t_{herd}} (\beta s(t) - \gamma) dt + \log \left(\frac{i_u(0)}{i_u(t_{herd})} \right) \\ &= \int_{t=0}^{t_{herd}} (\beta s(t) - \gamma) dt + \log \left(\frac{i_u(0)}{i_{\max}} \right), \end{aligned}$$

where we have used Lemma 4 for the last equality. Note that the second term is a constant and η is a positive constant. Therefore, the original optimal control problem can be rewritten as:

$$\begin{aligned} & \min \int_{t=0}^{t_{herd}} (\beta s(t) - \gamma) dt \\ \text{s.t.} \quad & i_u(t) \leq i_{\max} \quad \forall t \\ & \theta(t) \geq 0 \quad \forall t. \end{aligned} \tag{S2}$$

We next show that the trajectory i_u^\dagger induced by the control θ^\dagger pointwise dominates any other feasible trajectory i_u and therefore the corresponding trajectory s^\dagger is pointwise smaller than any other feasible trajectory of s , before hitting herd immunity (Fig. S1). This has two consequences: i) herd immunity is reached sooner under θ^\dagger and ii) $(\beta(t)s(t) - \gamma)$ is pointwise smaller. These two points prove that θ^\dagger minimizes Eq. (S2) and thus also Eq. (S1).

To prove points i) and ii) recall that from the first line of Eq. (1)

$$\frac{ds}{dt} = -\beta s i_u \quad \implies \quad \frac{1}{s} \frac{ds}{dt} = -\beta i_u \quad \implies \quad \frac{d \log(s)}{dt} = -\beta i_u$$

and by integration

$$\log \left(\frac{s(t)}{s(0)} \right) = - \int_0^t \beta(\tau) i_u(\tau) d\tau$$

which shows that for two feasible trajectories $(s^\dagger(t), i_u^\dagger(t))$ and $(s(t), i_u(t))$, if $i_u^\dagger(t) \geq i(t)$ for all $t \leq T$, we have that $s^\dagger(t) \leq s(t)$ for all $t \leq T$. \square

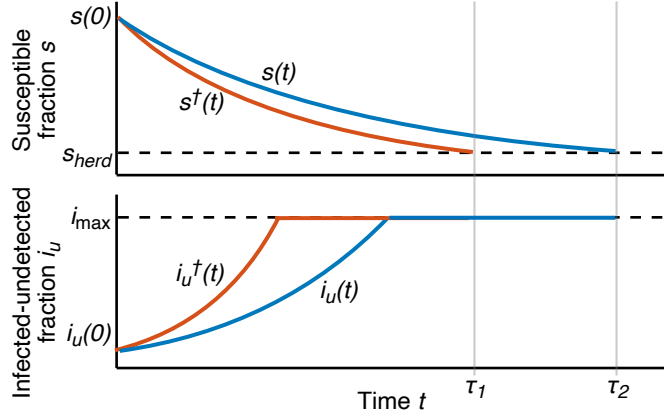


Figure S1: The trajectory $i_u^\dagger(t)$ induced by the optimal testing strategy θ^\dagger pointwise dominates any other feasible trajectory i_u . Conversely, the trajectory $s^\dagger(t)$ induced by the optimal testing strategy θ^\dagger is pointwise smaller than any other feasible trajectory $s(t)$, until herd immunity is reached. In this illustration β is constant, so that $s(t_{herd}) = \gamma/\beta = s_{herd}$.

Combining the lemmas above proves Theorem 2. The expression of θ^\dagger when $i_u(t) = i_{\max}$ can be obtained from $di_u/dt = (\beta s - \gamma - \eta\theta^\dagger)i_u = 0$.

S.2 Proofs of Observability

S.2.1 Proof of Lemma 1

We prove the two statements separately.

1. From the third line of Eq. (1), it holds

$$i_u(t) = \frac{1}{\eta\theta(t)} \left(\frac{di_d(t)}{dt} + \gamma i_d(t) \right)$$

hence i_u (and all its derivatives) can be reconstructed from the observed output i_d (and its derivative). From the second line of Eq. (1), for β constant, we obtain

$$\beta s(t) = \frac{1}{i_u(t)} \frac{di_u(t)}{dt} + \gamma + \eta\theta(t). \quad (\text{S3})$$

Substituting the expression in Eq. (S3) on the right hand side of

$$\beta = -\frac{1}{\beta s(t)i_u^2(t)} \left(\frac{d^2 i_u(t)}{dt^2} - \beta s(t) \frac{di_u(t)}{dt} + \gamma \frac{di_u(t)}{dt} + \eta \frac{d\theta(t)}{dt} i_u(t) + \eta\theta(t) \frac{di_u(t)}{dt} \right)$$

(obtained by computing the second derivative of i_d) yields a formula for β as a function of known quantities (i_u , i_d , θ and their derivatives). Since $\beta s(t)$ is known from Eq. (S3), this implies that $s(t)$ is known and finally $r(t) = 1 - s(t) - i_u(t) - i_d(t)$.

2. If $\beta(t)$ is time-varying the system is not observable. To show this we consider two evolutions that start from different initial conditions and have different β evolutions, yet lead to the same observable output i_d . This proves that just observing the output it is not possible to distinguish the two scenarios. Specifically consider the two systems:

$$\begin{cases} \frac{ds}{dt} = -\beta s i_u \\ \frac{di_u}{dt} = \beta s i_u - \gamma i_u - \eta \theta(t) i_u \\ \frac{di_d}{dt} = \eta \theta(t) i_u - \gamma i_d \end{cases} \quad \begin{cases} \frac{d\bar{s}}{dt} = -\bar{\beta} \bar{s} \bar{i}_u \\ \frac{d\bar{i}_u}{dt} = \bar{\beta} \bar{s} \bar{i}_u - \gamma \bar{i}_u - \eta \theta(t) \bar{i}_u \\ \frac{d\bar{i}_d}{dt} = \eta \theta(t) \bar{i}_u - \gamma \bar{i}_d \end{cases}$$

with initial state $s(0) \neq \bar{s}(0)$, $i_u(0) = \bar{i}_u(0)$, $i_d(0) = \bar{i}_d(0) = r(0) = \bar{r}(0) = 0$ and suppose that $\bar{\beta}(t) = \beta(t)s(t)/\bar{s}(t)$. Then

$$\begin{aligned} \frac{di_u}{dt} &= \beta s i_u - \gamma i_u - \eta \theta(t) i_u, \\ \frac{d\bar{i}_u}{dt} &= \beta s \bar{i}_u - \gamma \bar{i}_u - \eta \theta(t) \bar{i}_u, \quad \bar{i}_u(0) = i_u(0) \end{aligned}$$

Since i_u and \bar{i}_u solve the same differential equation it must be $\bar{i}_u(t) \equiv i_u(t)$ for all t . This immediately implies $i_d(t) \equiv \bar{i}_d(t)$, yet the evolution of s and \bar{s} is different as they start from different initial conditions.

S.2.2 Proof of Lemma 2

Since $y(t)$ is observed continuously in time one can use it to compute exactly di_d/dt and dr_d/dt . The third and fifth equations in Eq. (3) can then be used to recover $i_u(t)$ and $r(t)$ exactly as follows:

$$\begin{aligned} i_u(t) &= \frac{1}{\eta \theta(t) + \theta_B \eta_{BI}} \left(\frac{di_d}{dt} + \gamma i_d \right), \\ r_u(t) &= \frac{1}{\theta_B \eta_{BR}} \left(\frac{dr_d}{dt} - \gamma i_d \right). \end{aligned}$$

Using the fact that

$$s(t) = 1 - i_u(t) - r_u(t) - i_d(t) - r_d(t)$$

one can reconstruct $s(t)$ as well. Overall, the state can be estimated exactly from the observed variables. As a byproduct, knowledge of $s(t)$ and $i_u(t)$ allows the identification of $\beta(t)$ from the first equation in Eq. (3).

S.3 Optimal testing policy for the extended problem in Eq. 4

We consider an extension of the model in Eq. (3) that accounts for detection of symptomatic individuals by considering an additional flow from infected-undetected to infected-detected with rate κ :

$$\begin{aligned} \frac{ds(t)}{dt} &= -\beta(t)s(t)i_u(t) \\ \frac{di_u(t)}{dt} &= \beta(t)s(t)i_u(t) - \gamma i_u(t) - \eta \theta(t)i_u(t) - \kappa i_u(t) - \theta_B \eta_{BI} i_u(t) \\ \frac{di_d(t)}{dt} &= \eta \theta(t)i_u(t) + \kappa i_u(t) + \theta_B \eta_{BI} i_u(t) - \gamma i_d(t) \\ \frac{dr_u(t)}{dt} &= \gamma i_u(t) - \theta_B \eta_{BR} r_u(t) \\ \frac{dr_d(t)}{dt} &= \gamma i_d(t) + \theta_B \eta_{BR} r_u(t) \end{aligned} \tag{S4}$$

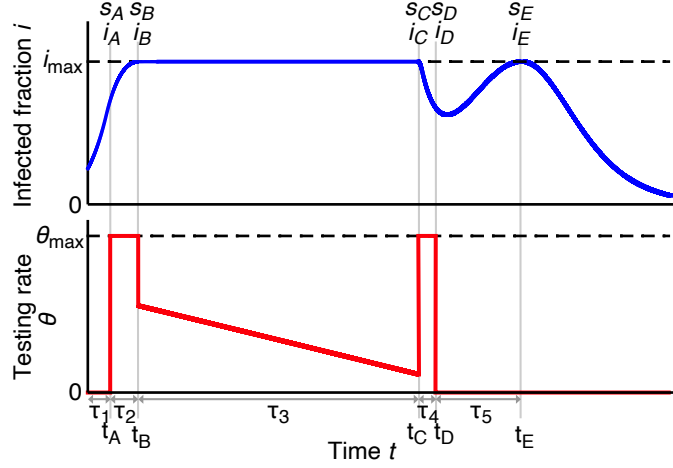


Figure S2: Structure of the optimal testing strategy (red curve) and corresponding effect on the total fraction of infected individuals (blue curve). The optimal testing policy $\hat{\theta}^*$ is zero until time t_A , when it switches to the maximum testing rate θ_{\max} until time t_B , when $i = i_u + i_d$ reaches the constraint i_{\max} with zero derivative. In the interval $[t_B, t_C]$ of duration τ_3 , the optimal testing policy maintains $i = i_{\max}$, until switching back to θ_{\max} between times t_C and t_D . After t_D , i increases until reaching i_{\max} with zero derivative at time t_E , and decreases afterwards.

The numerical solution of the problem in Eq. (4) for this extended model (and for the parameters of Fig. 4) has the structure described in Section 2.3 and schematized in Fig. S2. To generalize this analysis to any set of parameters, we here aim at deriving an analytic characterization of the optimal testing policy for Problem 4 within the class of policies with such a structure. More in detail, we aim at deriving analytic expressions for the optimal switching times t_A , t_B , t_C and t_D and for the testing rate in the interval $[t_B, t_C]$ as a function of the model parameters and initial conditions. With slight abuse of notation, we denote the optimal policy within this class with the symbol θ^* . For this analysis we assume β to be constant, and without loss of generality we assume $\eta = 1$. Moreover, we work under the assumption that the state is known, hence we set $\theta_B = 0$.

The following analytic relationships (adapted from [Harko et al., 2014]) between s and i_u at two times $t_1 < t_2$ under constant testing rate θ will be useful:

$$f_{\theta}(s(t_1), i_u(t_1), s(t_2), i_u(t_2)) := \ln \left(\frac{s(t_2)}{s(t_1)} \right) - \frac{\beta}{\gamma + \theta + \kappa} (s(t_2) + i_u(t_2) - s(t_1) - i_u(t_1)) = 0, \quad (\text{S5})$$

$$t_2 - t_1 = \int_{e^{-\frac{\beta}{\gamma + \theta + \kappa}(1 - s(t_1) - i_u(t_1))}}^{\frac{s(t_2)}{s(t_1)} e^{-\frac{\beta}{\gamma + \theta + \kappa}(1 - s(t_1) - i_u(t_1))}} \frac{1}{x - \beta - (\gamma + \theta + \kappa) \ln x + \beta s(t_1) x e^{\frac{\beta}{\gamma + \theta + \kappa}(1 - s(t_1) - i_u(t_1))}} dx := \Delta t_{\theta}(s(t_2), s(t_1), i_u(t_1)). \quad (\text{S6})$$

S.3.1 Intervals $[0, t_A]$ and $[t_A, t_B]$

First, we evaluate $s_A := s(t_A)$, $i_{uA} := i_u(t_A)$, $s_B := s(t_B)$ and $i_{uB} := i_u(t_B)$ as functions of s_0 and i_0 . Using Eq. (S5) we have:

$$f_0(s_0, i_0, s_A, i_{uA}) = 0, \quad (\text{S7})$$

$$f_{\theta_{\max}}(s_A, i_{uA}, s_B, i_{uB}) = 0. \quad (\text{S8})$$

Imposing that at time t_B one has $(i_u + i_d)|_{t_B} = i_{\max}$ and $d(i_u + i_d)/dt|_{t_B} = 0$ yields:

$$\left. \frac{d(i_u + i_d)}{dt} \right|_{t_B} = \beta s_B i_{uB} - \gamma(i_{uB} + i_d(t_B)) = \beta s_B i_{uB} - \gamma i_{\max} = 0, \quad (\text{S9})$$

and integrating $di_d/dt = (\theta_{\max} + \kappa)i_u - \gamma i_d$ in $[t_A, t_B]$ one finds:

$$\begin{aligned} i_{dB} &= i_{\max} - i_{uB} = \left(i_{dA} + (\theta_{\max} + \kappa) \int_{t_A}^{t_B} e^{\gamma(t-t_A)} i_u(t) dt \right) e^{-\gamma(t_B-t_A)} \\ &= \left(i_{dA} + (\theta_{\max} + \kappa) \int_{s_A}^{s_B} e^{\gamma \Delta t_{\theta_{\max}}(s, s_A, i_{uA})} i_u(s) \frac{dt}{ds} ds \right) e^{-\gamma \tau_2} \\ &= \left(i_{dA} + (\theta_{\max} + \kappa) \int_{s_B}^{s_A} \frac{e^{\gamma \Delta t_{\theta_{\max}}(s, s_A, i_{uA})}}{\beta s} ds \right) e^{-\gamma \tau_2}, \end{aligned} \quad (\text{S10})$$

where τ_2 can be computed from Eq. S6 as a function of s_A , i_{uA} and s_B . The quantity i_{dA} can be computed as a function of s_A by integrating $di_d/dt = -\gamma i_d + \kappa i_u$ in the interval $[0, t_A]$, which gives:

$$i_{dA} = e^{-\gamma t_A} \int_{s_A}^{s_0} e^{\gamma \Delta t_0(s, s_0, 0)} \frac{\kappa}{\beta s} ds,$$

where again we made use of Eq. S6. Eqs. (S7)-(S10) are four equations in four unknowns that can be solved to find s_A, i_{uA}, s_B, i_{uB} as a function of s_0 and i_0 . In the interval $[t_A, t_B]$, the optimal testing policy is $\theta^*(t) = \theta_{\max}$, and thus the cost of the control in the interval $[0, t_B]$ is:

$$\int_0^{t_B} \theta^*(t) dt = \tau_2 \theta_{\max}.$$

S.3.2 Interval $[t_B, t_C]$

In the interval $[t_B, t_C]$ the optimal testing policy maintains $i = i_u + i_d \equiv i_{\max}$. Hence, the first and second derivatives of i must be equal to zero. Note that

$$\begin{aligned} \frac{d(i_u + i_d)}{dt} &= \beta s i_u - \gamma(i_u + i_d) = \beta s i_u - \gamma i_{\max} = 0 \\ \frac{d^2(i_u + i_d)}{dt^2} &= \beta \frac{ds}{dt} i_u + \beta s \frac{di_u}{dt} = \beta(-\beta s i_u) i_u + \beta s (\beta s i_u - \gamma i_u - \theta^* i_u - \kappa i_u) \\ &= -\beta^2 s i_u^2 + \beta^2 s^2 i_u - \beta s \gamma i_u - \beta s \theta^* i_u - \beta \kappa s i_u = 0 \end{aligned}$$

which yields

$$\theta^* = \beta(s - i_u) - \gamma - \kappa. \quad (\text{S11})$$

Substituting this expression in the dynamic equations, we obtain that in the interval $[t_B, t_C]$ the undetected fraction of the infected individuals satisfies:

$$\frac{di_u}{dt} = (\beta s - \gamma - \theta^* - \kappa) i_u = \beta i_u^2 \quad (\text{S12})$$

and thus

$$i_u(t) = \frac{1}{\frac{1}{i_{uB}} - \beta(t - t_B)}. \quad (\text{S13})$$

Moreover,

$$\begin{aligned} \frac{di_d}{dt} &= \theta^* i_u + \kappa i_u - \gamma i_d = \beta s i_u - \gamma i_u - \beta i_u^2 - \gamma i_d = -\frac{ds}{dt} - \gamma i_u - \frac{di_u}{dt} - \gamma i_d \\ \Rightarrow 0 &= \frac{di_u}{dt} + \frac{di_d}{dt} = -\frac{ds}{dt} - \gamma(i_u + i_d) \Rightarrow \frac{ds}{dt} = -\gamma i_{\max} \\ \Rightarrow s(t) &= s_B - \gamma i_{\max}(t - t_B). \end{aligned} \quad (\text{S14})$$

Thus, $s_C = s_B - \gamma i_{\max} \tau_3$ and $i_{uC} = 1/(1/i_{uB} - \beta \tau_3)$. The value of τ_3 is limited from above by the constraints $\tau_3 < (\beta i_{uB})^{-1}$ (for solvability of Eq. (S12)) and $\theta^* \geq 0$, which can be expressed as an upper constraint on τ_3 via Eqs. (S11), (S13) and (S14). We denote by $\bar{\tau}_3$ the minimum of such constraints. The cost of the optimal testing policy in the interval $[t_B, t_C]$ is:

$$\begin{aligned} \int_{t_B}^{t_C} \theta^*(t) dt &= \int_{t_B}^{t_C} (\beta(s(t) - i_u(t)) - \gamma - \kappa) dt \\ &= \int_0^{\tau_3} \left(\beta \left(s_B - \gamma i_{\max} t' - \frac{1}{\frac{1}{i_{uB}} - \beta t'} \right) - \gamma - \kappa \right) dt' \\ &= \tau_3 \left(\beta s_B - \gamma - \kappa - \frac{\gamma}{2} \beta i_{\max} \tau_3 \right) + \ln(1 - \beta i_{uB} \tau_3). \end{aligned}$$

S.3.3 Intervals $[t_C, t_D]$ and $[t_D, t_E]$

The analysis is identical to that of Section S.3.1, the objective is to evaluate s_D , i_{uD} , s_E and i_{uE} as a function of s_C and i_C . From Eq. (S5) we have:

$$\begin{aligned} f_{\theta_{\max}}(s_C, i_{uC}, s_D, i_{uD}) &= 0 \\ f_0(s_D, i_{uD}, s_E, i_{uE}) &= 0. \end{aligned}$$

At time t_E , $i_u + i_d$ is tangent to i_{\max} , hence: (similar to Eq. (S9))

$$\beta s_E i_{uE} = \gamma i_{\max}.$$

Integrating $di_d/dt = \theta_{\max} i_u + \kappa i_u - \gamma i_d$ in the interval $[t_C, t_D]$ yields:

$$i_d(D) = \left(i_d(C) + (\theta_{\max} + \kappa) \int_{s_D}^{s_C} \frac{e^{\gamma \Delta t_{\theta_{\max}}(s, s_C, i_C)}}{\beta s} ds \right) e^{-\gamma \tau_4},$$

where $i_d(C) = i_{\max} - i_{uC}$. We can also compute $i_d(D)$ from the equation for i_d in the interval $[t_D, t_E]$ (during which the testing rate is equal to zero) as:

$$i_d(D) = (i_{\max} - i_{uE}) e^{\gamma \tau_5} - \kappa \int_{s_E}^{s_D} \frac{e^{\gamma \Delta t_0(s, s_D, i_D)}}{\beta s} ds,$$

and equating the two expressions for $i_d(D)$ we find:

$$(i_{\max} - i_{uE}) e^{\gamma \tau_5} - \kappa \int_{s_E}^{s_D} \frac{e^{\gamma \Delta t_0(s, s_D, i_D)}}{\beta s} ds = \left(i_{\max} - i_{uC} + (\theta_{\max} + \kappa) \int_{s_D}^{s_C} \frac{e^{\gamma \Delta t_{\theta_{\max}}(s, s_C, i_C)}}{\beta s} ds \right) e^{-\gamma \tau_4},$$

The time intervals τ_4 and τ_5 can be computed from Eq. (S6). The cost of the control in the interval $[t_C, +\infty]$ is thus:

$$\int_{t_C}^{\infty} \hat{\theta}^*(t) dt = \tau_4 \theta_{\max}.$$

S.3.4 Minimization over τ_3 yields the optimal testing policy

So far we obtained a formula for the overall cost that, for fixed s_0 and i_0 , depends only on τ_3 . Minimizing such cost for $\tau_3 \in [0, \bar{\tau}_3]$ yields the optimal value for τ_3 (Fig. S3), with which the optimal testing strategy θ^* is characterized. Note that since s is monotonically decreasing, the testing strategy can be formulated as follows:

$$\theta^*(t) = \begin{cases} 0 & \text{if } s(t) > s_A \text{ or } s(t) < s_D \\ \theta_{\max} & \text{if } s(t) \in [s_B, s_A] \cup [s_D, s_C] \\ \beta(s(t) - i_u(t)) - \gamma - \kappa & \text{otherwise} \end{cases}$$

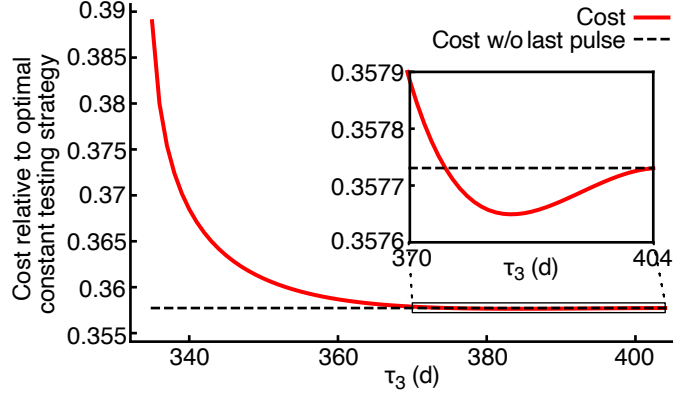


Figure S3: Cost of testing policies (red curve) with the structure of Fig. S2 for the deterministic SIR model Eq. (S4), as a function of the duration τ_3 of the time interval $[t_B, t_C]$. Costs are computed relative to the cost of the optimal, constant testing strategy (Materials and Methods Section 4.2). The optimal testing policy adopts the value of τ_3 that minimizes the cost (inset). The dashed, black line indicates the cost of a testing policy with the largest possible value of τ_3 , i.e. a testing policy in which the last phase of testing at maximum testing rate θ_{\max} does not occur. The inset shows that the benefit of the last phase of testing at maximum testing rate is marginal.

S.4 Receding horizon implementation of the optimal testing policy for the stochastic simulations

In the receding horizon implementation, at any time $t > t_A$ we aim at computing the testing rate $\theta_{rh}(t)$ that brings the deterministic dynamics of Eq. (S4) to $i_u + i_d = i_{\max}$ with $d(i_u + i_d)/dt = 0$ in a time H . This leads to the following set of equations:

$$\begin{aligned}
 f_{\theta_{rh}(t)}(s(t), i_u(t), s(t+H), i_u(t+H)) &= 0 \\
 \left. \frac{d(i_u(t) + i_d(t))}{dt} \right|_{t+H} &= \beta s(t+H) i_u(t+H) - \gamma i_{\max} = 0 \\
 s(t+H) &= s(t) - \beta \int_t^{t+H} s(t') i_u(t') dt' \simeq s(t) - \frac{\beta}{2} (s(t+H) i_u(t+H) + s(t) i_u(t)) H,
 \end{aligned} \tag{S15}$$

where f_{θ} is as in Eq. (S5) and in the last equation we used the trapezoidal rule to approximate the integral. We denote the solution of Eq. (S15) as:

$$\theta_{rh}(s(t), i_u(t)) := -\beta \frac{s(t) + i_u(t) - s(t+H)}{\ln(s(t+H)/s(t))} + \frac{\gamma i_{\max}}{s(t+H) \ln(s(t+H)/s(t))}. \tag{S16}$$

S.5 Validation with time-varying transmission rate

Fig. S4 illustrates the performance of the testing policy $\hat{\theta}^*$ for the optimization problem of Eq. 4 when the transmission rate is time-varying (in this case sinusoidal to mimic seasonality). For any time t , the transmission rate $\beta(t)$ is estimated from the reconstructed state $[\hat{x}(\tau)]_{\tau=t-7}^{t-1}$ over a moving window of length 7 days by nonlinear least square regression. The testing rate is evaluated by using Eqs. (14) and (S16) with the estimated $\hat{\beta}(t)$ instead of β . We see from Fig. S4 that the time-varying transmission rate can be accurately predicted (while the epidemic is active) and the testing rate implemented using such prediction effectively stabilizes the epidemics at the desired threshold. This is a preliminary indication that the suggested testing strategy may be effective even in the presence of an unknown and time-varying transmission rate. A detailed numerical study is needed to further support this conclusion and is left as future work.

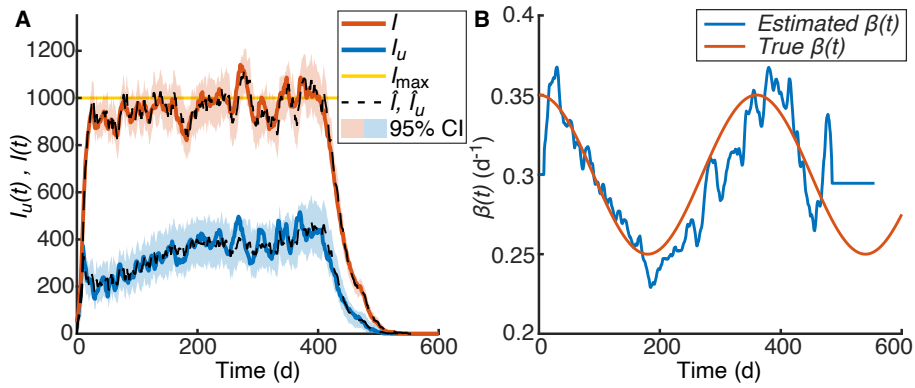


Figure S4: Performance of the testing policy $\hat{\theta}^*$ when $\beta(t)$ varies sinusoidally with a one year period centered at $\beta = 0.3 \text{ d}^{-1}$ and amplitude 0.1 d^{-1} . At any time t_k , $\beta(t_k)$ was estimated using data from the previous 7 days by fitting the epidemiological dynamics to the deterministic SIR model, taking into account the testing rates adopted. Panel A shows the total number of infected I (orange curve) and infected-undetected (blue curve) in a stochastic realization of the epidemic, along with the state estimates obtained from the extended Kalman filter (dashed, black curves). Panel B shows the true (orange curve) and estimated (blue curve) values of β .